

## Authors' Answers to the Referees' Comments

The authors thank the referees for their useful comments and suggestions to improve the clarity and readability of the paper. In the following we reply to their comments:

### Referee #1

#### General Comment :

The authors should make a stronger case earlier in the article.

Reply:

We added a sentence on page 7242, line 11 to indicate that we plan to use the new formalism to obtain the quantum yields for the isotopologue CHDO.

#### General Comment :

I suggest the authors include both the 2006 and 2013 IUPAC recommendations.

Reply:

The 2013 IUPAC recommendations are included in all relevant figures and in the discussion.

#### General Comment :

There is a degree of redundancy. Some consolidation would be helpful.

Reply:

All tables except Table 4 are omitted and the  $1\sigma$  errors included in the respective equations.

#### Specific Comment p.7242, l.5 :

Express as summation, with the A parameter a signed quantity?

Reply:

On page 7242, line 4 we replaced 'combination' by 'sums'. This should make clear what is meant.

#### Specific Comment p.7242, l.13 :

The criteria for rejecting some measurements are unclear

Reply:

We changed that sentence by specifying the criteria for rejecting measurements. We also listed explicitly the measurements not included.

Specific Comment p.7243, l.121 :

typo – ‘wavelength’

Reply:

corrected

Specific Comments p.7243, l.26 and p.7247, l.13 :

‘heat of formation’ should be ‘heat of reaction’

Reply:

changed

Specific Comment p.7242, l.5 :

Invoking a threshold for three-body dissociation does not help to explain the apparent decrease in the photolysis quantum yield.

Reply:

We agree, nevertheless we find the coincidence interesting.

Specific Comment p.7248, l.6 :

Equation (7) seems superfluous.

Reply:

We agree and omitted the equation.

Specific Comment p.7250, l.9 :

Replace ‘frequencies’ with ‘rates’.

Reply:

The term ‘photolysis frequency’ is generally used in our field. For consistency we prefer to keep it here, too.

Specific Comment p.7251, l.5 :

Equations 11 – 13 do not appear in the manuscript.

Reply:

The Table 1 (formerly Tab.4) with these equations (now numbered 8 to 10) is included in the text in due place.

Specific Comment p.7251, l.15-25 :

- (1) The effect of the temperature dependence of the absorption cross section should be addressed.
- (2) The variations of -9% and +6% in  $j_{\text{rad}}$  and  $j_{\text{mol}}$  are described as a significant effect. This seems inconsistent with the comment on page 7244, line 19-24. Why is -4% small, but +6% significant?

Reply:

- (1) Its effect on the  $j_i$  is small, less than 0.3 % for  $j_{\text{rad}}$  and less than 3% for  $j_{\text{tot}}$  and included in the calculation. We added a sentence (page.7250, line15) to indicate the size of the effect.
- (2) To resolve the apparent inconsistency we have changed the text on page 7244, line23 to indicate that the superposition of the line at 321 nm from Tatum Ernest et al. (2012) on our  $\Phi_{\text{rad}}$ , Eq.(3), would cause an increase in  $j_{\text{mol}}$  by less than 2 % at all altitudes and a decrease in  $j_{\text{rad}}$  by less than 4 %. These upper limits are more than a factor of 2 smaller than the changes of +6 % and - 9 % for  $j_{\text{mol}}$  and  $j_{\text{rad}}$  at 15 km altitude due to the assumed temperature dependence of  $\Phi_{\text{rad}}$ .

Specific Comment p.7262 :

typo 'Gratien' in figure caption

Reply:

corrected.

## **Referee #2**

General Comment :

The discussion of the quantum yield temperature dependence and its impact on atmospheric photolysis rates seems out of place.

Reply:

The idea is to show the impact of a possible temperature dependence of  $\Phi_{\text{rad}}$  on  $j_{\text{rad}}$  and  $j_{\text{mol}}$  to see whether that effect is significant and needs further attention.

Comment p.7264, Figure 4 :

It would be very instructive to include an additional panel that shows the wavelength dependence of the product of the terms shown in this figure.

Reply:

The product is included.

Technical Comment p.7240, l.1:

delete 'various'

Reply:

deleted

Technical Comment p.7240, equations :

It would be useful to provide the photolysis threshold wavelengths (energies) along with the possible photolysis channels.

Reply:

We prefer to introduce the photolysis thresholds in the respective section where they are needed.

Technical Comment p.7241 :

Fluorescence is noted here to account for a small yield in the photolysis of CH<sub>2</sub>O. I suggest the authors reconsider their decision to neglect fluorescence even if only a minor term.

Reply:

Given the experimental uncertainties in the  $\Phi_i$  which are on the order of 10 %, our formalism does not include effects which amount to a few % corrections, such as the line structure in  $\Phi_{rad}$  by Tatum Ernest et al. (2012) or here the fluorescence. But they are mentioned in the text to inform the reader.

Technical Comment p.7242, l.3: :

'a more handy tool ...': The proposed parametrization is more physically based, but not necessarily easier to implement.

Reply:

We changed the sentence on line 2 to make clear that the fourth order polynomial exists only for  $\Phi_{rad}$ . We are of the opinion that the fit by a functional term is more handy than a look-up table.

Technical Comment p.7243, l.5 :

delete 'without any weighing'

Reply:

deleted

Technical Comment p.7243, l.12 :

wavelengths

Reply:

corrected

Technical Comment p.7244, l.9 :

delete 'Discussion'

Reply:

deleted

Technical Comment p.7246, l.1 :

'vanishes' poor wording

Reply:

We prefer to keep 'vanishes'

Technical Comment p.7249 :

equations 11 – 13 do not exist in the paper

Reply:

The Table 1 (formerly Tab.4) with these equations (now numbered 8 to 10) is included in the text in due place.

### **Referee #3**

Comment p.7242, l.12-16 and p.7243,l.3-14

The authors should discuss in more detail their selection criteria and should incorporate the recent high structured QY data of Tatum Ernest et al. (2012) in their analysis.

Reply:

We changed that sentence on page7242, line13 by specifying the criteria for rejecting measurements. We also listed explicitly the measurements not included. We also

added a sentence on page7242, line23 that quantify the effect of a superposition of the line at 321 nm from Tatum Ernest et al. on our Eq.(3) for  $\Phi_{\text{rad}}$  on the photolysis rates in the atmosphere. (see reply to Referee #1)

Comment p.7243,l. 10-17 and Fi.1 to 3

- (1) It is not clear from the text if the fit shown in Fig.1 represents Eq.(3) or Eq.(11) of Table 4.
- (2) Is it possible to improve the fitting at the plateau and tail of the QY curve of Fig.1 ?

Reply:

- (1) The respective equations are now added to the legends.
- (2) As we discussed in the text on page7244, line17, there is the possibility to improve the fitting by a wavelength-dependent parameter b, once sufficiently accurate data become available. Another possibility was applied by Troe (2007) who multiplied the QY by a function of the type of Eq.(2). If the tail is cut off at 340 nm, the photolysis frequency is diminished by less than 10 % at all altitudes.

Comment p.7245, l.10

What is the correlation coefficient for IUPAC 2013 ?

Reply:

The coefficient of determination is added to the text, its value is 0.876.

Comment p.7248, l.6-11

It would be interesting to graphically compare the QY curves obtained by the individual Eqs.(3), (4), and (6) with the QY curves obtained by the simultaneous fit of Eqs. (11)-(13). Moreover it would be advantageous to list the recommended QY from Eqs. (11) to (13) in tabular form.

Reply:

We prefer to keep the figures as they are, further addition of curves would make them rather busy.

Comment p.7250, l.14

Preferably another reference should be used for Gratien et al. (2007)

Reply:

We changed the reference.

Comment p.7251, l.5

What is the resolution of the formaldehyde absorption cross section used? Have the authors considered using other available absorption spectra at higher resolution?

Reply:

All calculations were carried out with a resolution of 1 nm, as now mentioned in the text on page 7251, line 17. To check the influence of the absorption cross section's resolution we used the high resolution formaldehyde spectrum of Meller and Moortgat (2000) with a resolution of 0.01 nm. First, we calculated the photolysis frequencies with original spectrum and then with the cross sections integrated over 1 nm. The differences in the  $j_i$  are less than 0.1 %, i.e. in the range of the numerical errors.

Comment p.7252, l.9-24 and Fig.6

It would be useful to include the calculation of the  $j$  values in Fig.6 using the QY data of IUPAC 2013.

Reply:

These calculations are added in the text and in Fig.6.

Typos and Corrections

Reply:

Typos are corrected.

## 1 **List of Relevant Changes**

### 2 A simple formulation of the CH<sub>2</sub>O photolysis quantum yields

3 E.-P. Röth<sup>1</sup> and D. H. Ehhalt<sup>2</sup>

4

5 The following changes were made in the text (referring to the marked-up manuscript) :

6

7 page 2 / line 25

8 For  $\Phi_{\text{rad}}$  also a fit by a fourth order polynomial (see Sander et al., 2011) exists. To provide a

9 more handy tool for atmospheric modeling we propose to use sums of energy dependent

10 functions of the type

$$11 \quad \frac{A}{1+\exp\left[\frac{-(1/\lambda-1/\lambda_0)}{b}\right]} \quad (2)$$

12 to fit  $\Phi_{\text{mol}}$  and  $\Phi_{\text{rad}}$ .

13

14 page 3 / line 1

15 In particular we hope to eventually construct expressions of the quantum yields for CHDO for

16 which –apart from the threshold energies and a few isotope fractionation factors- no direct

17 measurements exist.

18

19 page 3 / line 4 - 13

20 Our analysis of the quantum yields will be based on the data filed by JPL (Sander et al., 2011)

21 and IUPAC (2006) omitting all measurements whose wavelength dependencies deviate

22 strongly from the forms recommended by JPL or IUPAC (e.g. McQuigg and Calvert, Clark et

23 al., Tang et al. for  $\Phi_{\text{rad}}$ ). Likewise, if measured data appear in several publications by the same

24 authors, only the latest data were considered. Not all data are independent of each other, as

25 some measurements (Smith et al., 2002, Pope et al., 2005, Tatum Ernest et al., 2012) are

26 relative and normalized to absolute quantum yields (DeMore et al., 1997, Sander et al., 2011).

27 This influences the uncertainty range of the parameters  $A_i$  whose  $1\sigma$  errors might be

28 somewhat larger than indicated in the respective equations.

29

30 page 5 / line 2

31 As Tatum Ernest et al. (2012) already indicated even the strong feature in  $\Phi_{\text{rad}}$  at 321 nm

32 produces only a small change in the photolysis frequencies in the atmosphere. In fact

33 superposition of this feature on Equation 3 would increase  $j_{\text{mol}}$  by less than 2 % at all altitudes



1 and decrease  $j_{\text{rad}}$  by less than 4%, because it coincides with a small value in the absorption  
2 coefficient of  $\text{CH}_2\text{O}$ .

3

4 page 9 / line 28

5 Its effect on the  $j_i$  is quite small – e.g. less than 0.3 % for  $j_{\text{rad}}$  – and included in the  
6 calculations.

7

8 page 10 / line 11

9 The curve for  $\sigma \cdot \Phi \cdot F_\lambda$  in Fig.4 nicely illustrates why the line structure observed by Tatum  
10 Ernest et al. (2012) at 321 nm has so little impact on  $j_{\text{mol}}$ : It would increase the quite small  
11 feature at 321 nm in that product by only a factor of 1.5.

12

13 page 10 / line 17

14 The calculations were made with 1 nm spectral resolution and are shown in Figure 5.

15

16 page 12 / added or changed references

17 Clark, J. H., Moore, C. B., and Nogar, N. S.: The photochemistry of formaldehyde: Absolute  
18 quantum yields, radical reactions, and NO reactions, *J. Chem. Phys.*, 68, 1264 - 1271, 1978  
19 DeMore, W. B., Sander, S. P., Howard, C. J., Ravishankara, A. R., Golden, D. M., Kolb, C.  
20 E., Hampson, R. F., Kurylo, M. J., Molina, M. J.: NASA panel for data evaluation, chemical  
21 kinetics and photochemical data evaluation for use in stratospheric modeling, JPL Publication  
22 97-4, 1997

23 Gratien, A., Nilsson, E., Doussin, J.-F., Johnson, M. S., Nielsen, C. J., Stenstrom, Y., and  
24 Picquet-Varrault, B.: UV and IR absorption cross-sections of HCHO, HCDO, and DCDO, *J.*  
25 *Phys. Chem. A*, 111, 11506 - 11513, 2007

26 McQuigg, R. D. and Calvert, J. G.: The photodecomposition of  $\text{CH}_2\text{O}$ ,  $\text{CD}_2\text{O}$ ,  $\text{CHDO}$ , and  
27  $\text{CH}_2\text{O}-\text{CD}_2\text{O}$  mixtures at Xenon flash lamp intensities, *J. Am. Chem. Soc.*, 91, 1590 – 1599,  
28 1969

29 Tang, K. Y., Fairchild, P. W., and Lee, E. K. C.: Laser-induced photodecomposition of  
30 formaldehyde ( $A^1A_2$ ) from its single vibronic levels. Determination of the quantum yield of H  
31 atom by  $\text{HNO}^*$  ( $A^1A''$ ) chemiluminescence, *J. Phys. Chem.*, 83, 569 – 573, 1979

32

33

34 changes in tables and figures

1  
2  
3  
4

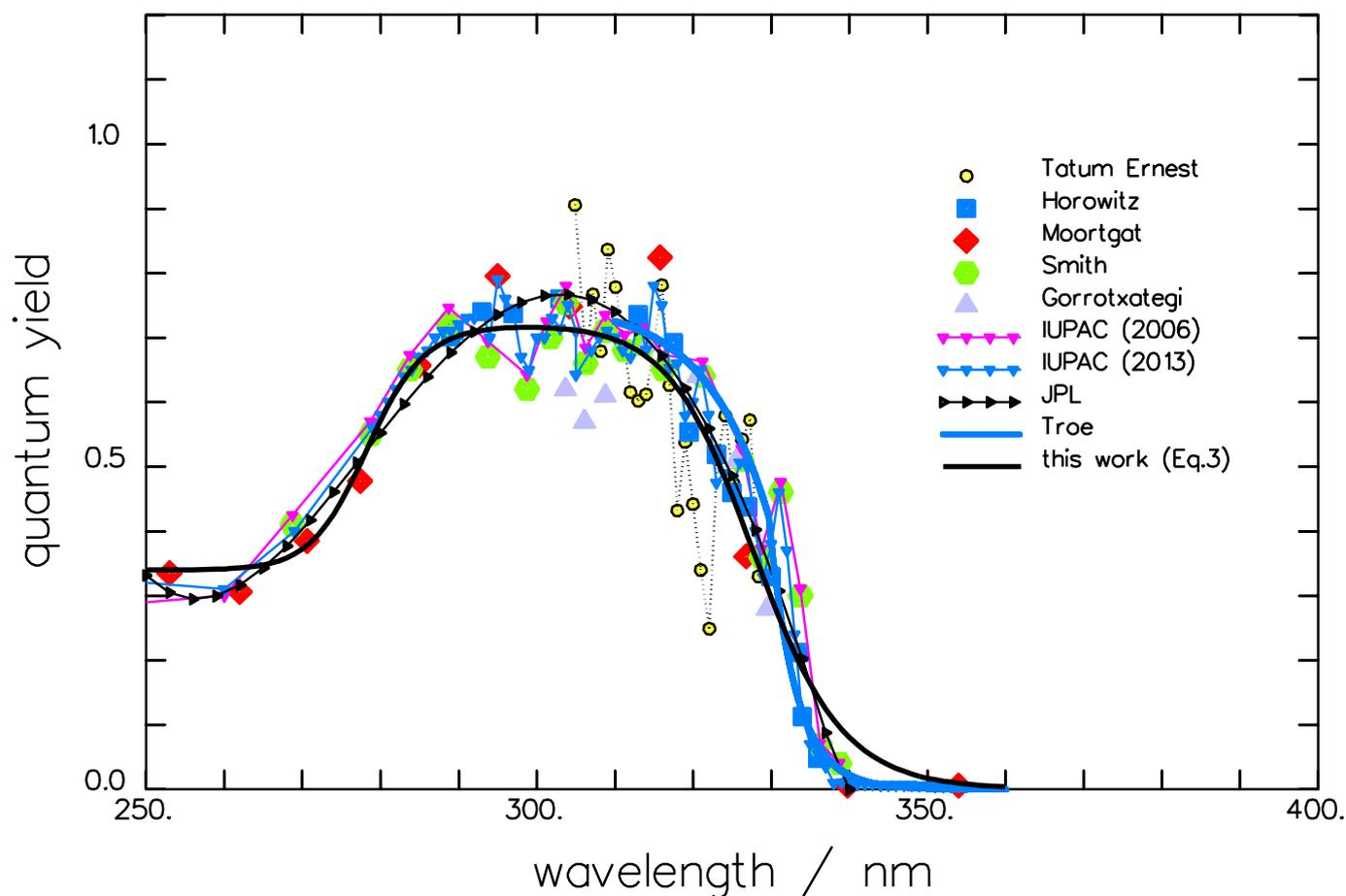
**Table 1:** Recommended quantum yield functions for use in atmospheric chemistry models (wavelength  $\lambda$  in nm).

$$\Phi_{rad} = \frac{0.74 \pm 0.01}{1 + \exp\left(\frac{-\left(\frac{1}{\lambda} - \frac{1}{327.4 \pm 0.5}\right)}{(5.4 \pm 0.5) \cdot 10^{-5}}\right)} - \frac{0.40 \pm 0.04}{1 + \exp\left(\frac{-\left(\frac{1}{\lambda} - \frac{1}{279.0 \pm 1.3}\right)}{(5.2 \pm 2.4) \cdot 10^{-5}}\right)} \quad (8)$$

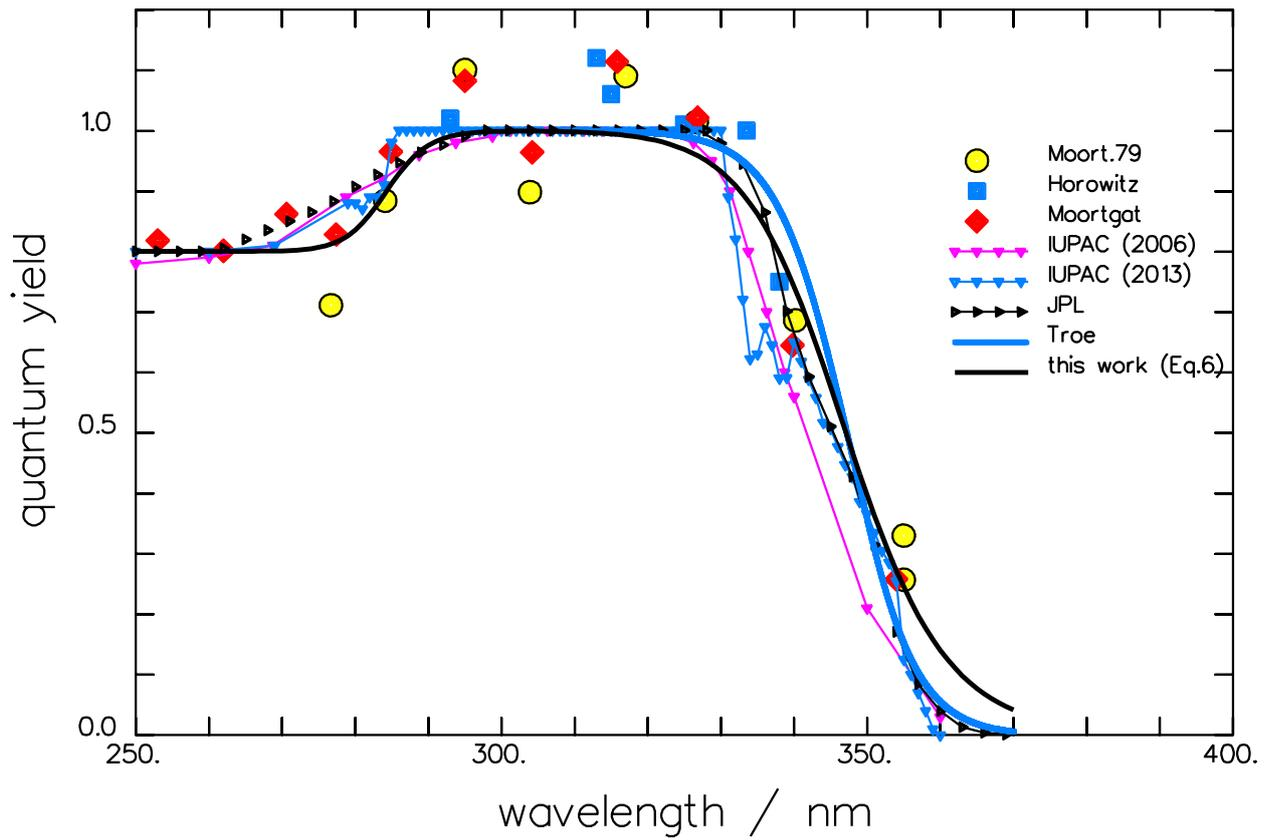
$$\Phi_{tot} = \frac{1}{1 + \exp\left(\frac{-\left(\frac{1}{\lambda} - \frac{1}{346.9 \pm 0.5}\right)}{(5.4 \pm 0.3) \times 10^{-5}}\right)} (M/M_0) - \frac{0.22 \pm 0.02}{1 + \exp\left(\frac{-\left(\frac{1}{\lambda} - \frac{1}{279.0 \pm 1.3}\right)}{(5.2 \pm 2.4) \times 10^{-5}}\right)} \quad (9)$$

$$\Phi_{mol} = \frac{1}{1 + \exp\left(\frac{-\left(\frac{1}{\lambda} - \frac{1}{346.9 \pm 0.5}\right)}{(5.4 \pm 0.3) \times 10^{-5}}\right)} (M/M_0) - \frac{0.74 \pm 0.01}{1 + \exp\left(\frac{-\left(\frac{1}{\lambda} - \frac{1}{327.4 \pm 0.5}\right)}{(5.4 \pm 0.5) \cdot 10^{-5}}\right)} + \frac{0.18 \pm 0.02}{1 + \exp\left(\frac{-\left(\frac{1}{\lambda} - \frac{1}{279.0 \pm 1.3}\right)}{(5.2 \pm 2.4) \cdot 10^{-5}}\right)} \quad (10)$$

5  
6  
7

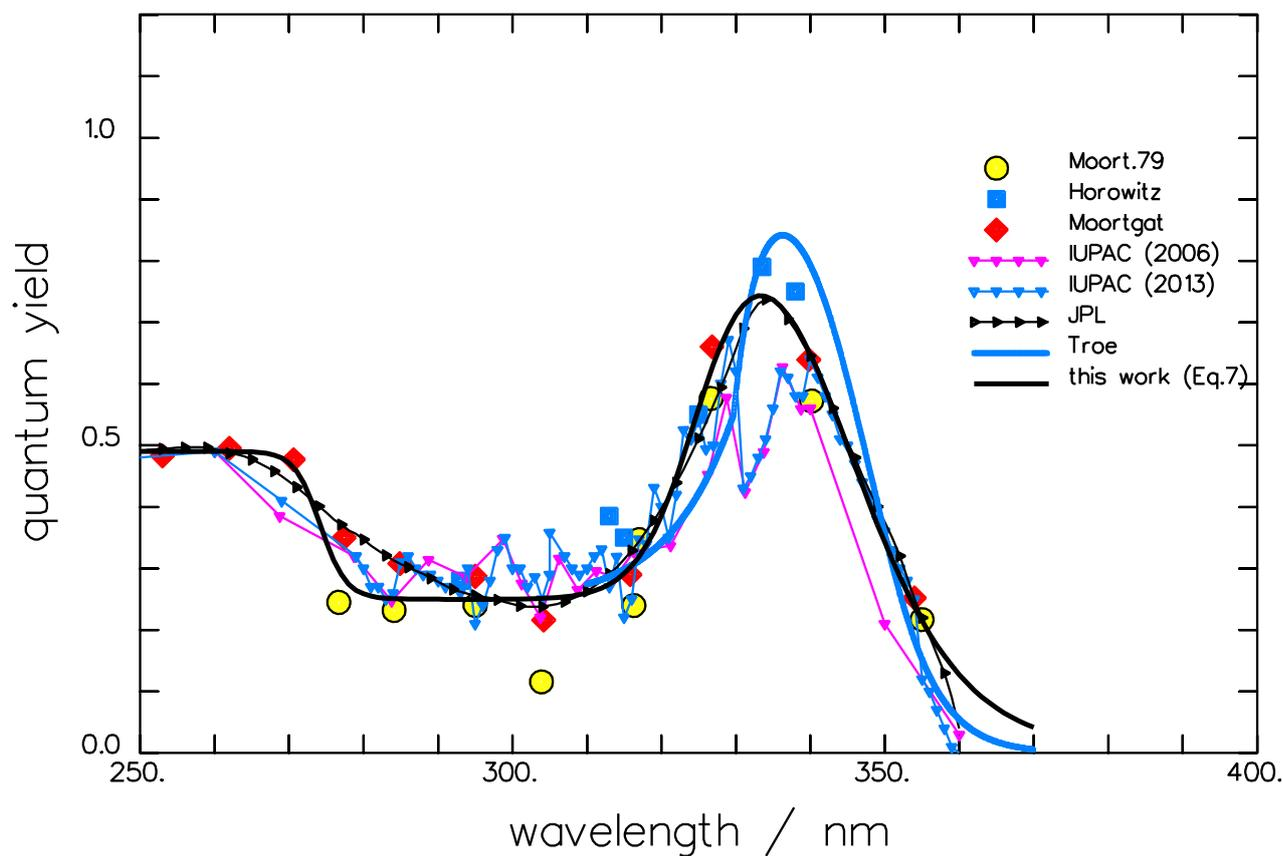


1  
2  
3  
4 **Figure 1:** Spectrum of the quantum yield of the radical channel of the CH<sub>2</sub>O photolysis at  
5 room temperature. Measured data used for the fit are indicated by the large full symbols  
6 (**Horowitz** and Calvert, 1978; **Moortgat** et al., 1983; **Smith** et al., 2002; **Gorrotxategi**  
7 Carbajo et al., 2008). The present fit and the theoretical curve from **Troe** (2007) are given by  
8 full lines. Recommended data are represented by small symbols connected by a thin line: **JPL**  
9 (Sander et al., 2011); **IUPAC (2006)**, and **IUPAC (2013)**. The line structure observed by  
10 **Tatum Ernest** et al. (2012) is indicated by open circles and a dotted line.  
11



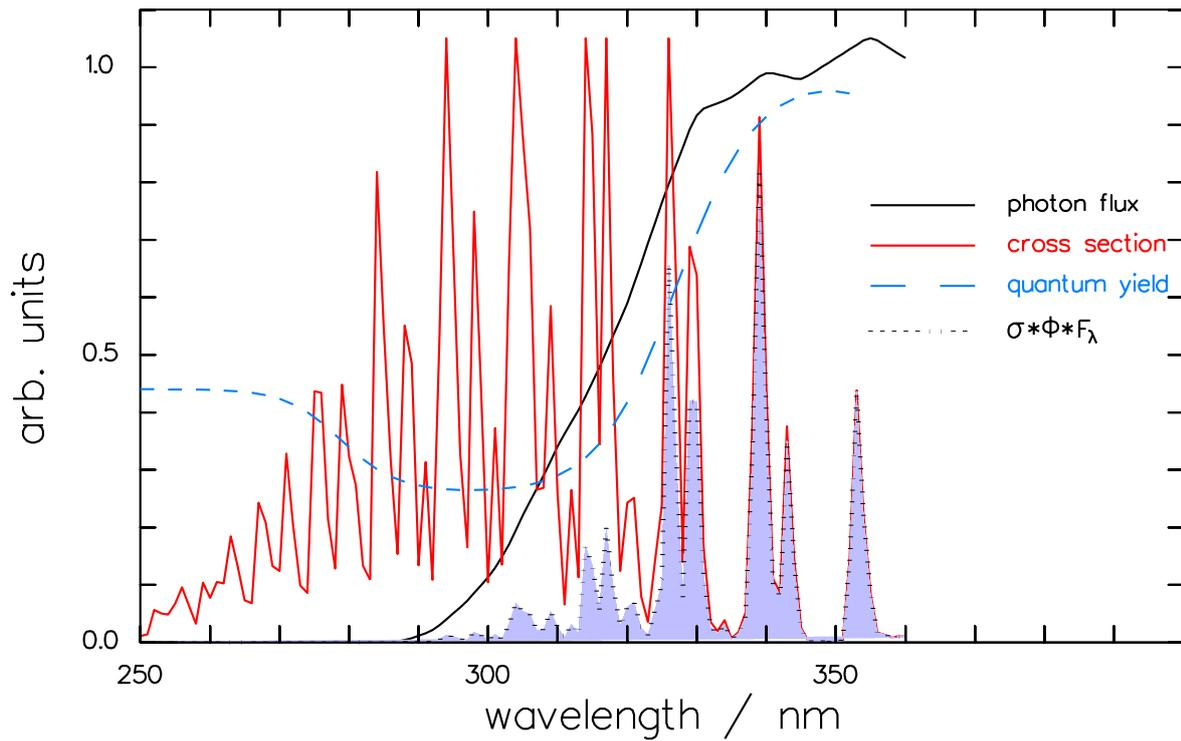
1  
2  
3  
4  
5  
6  
7  
8  
9  
10  
11

**Figure 2:** Spectrum of the quantum yield of the total CH<sub>2</sub>O photolysis at room temperature. Measured data used for the fit are indicated by the large full symbols (**Moort.79:** Moortgat and Warneck, 1979, **Horowitz** and Calvert, 1978; **Moortgat** et al., 1983). The present fit and the theoretical curve from **Troe** (2007) are given by full lines. Recommended data are represented by small symbols connected by a thin line: **JPL** (Sander et al., 2011); **IUPAC (2006)**, and **IPUAC (2013)**.



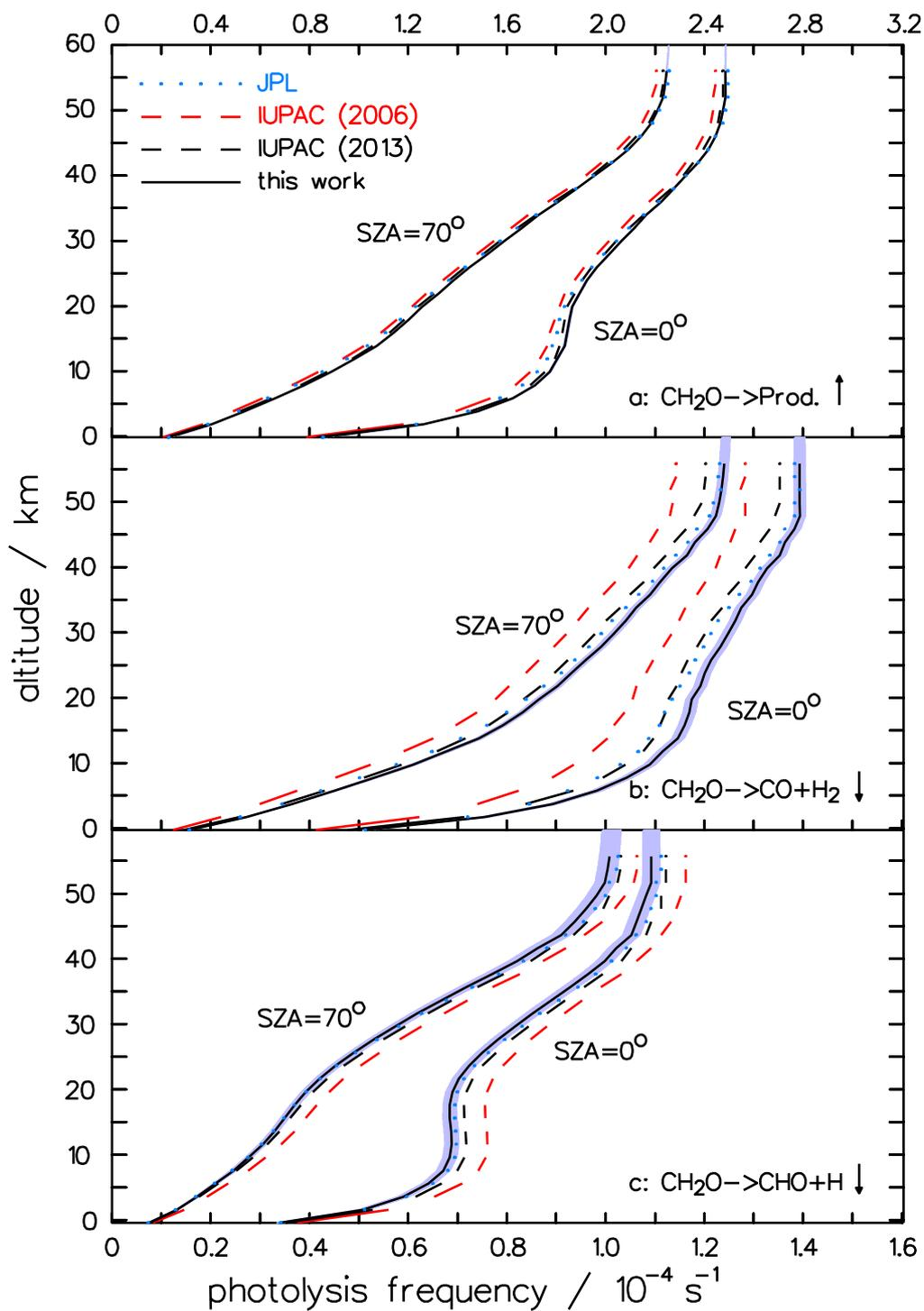
1  
2  
3  
4  
5  
6  
7  
8  
9  
10  
11

**Figure 3:** Spectrum of the quantum yield of the molecular branch of the  $\text{CH}_2\text{O}$  photolysis at room temperature. Measured data used for the fit are indicated by the large full symbols (**Moort.79:** Moortgat and Warneck, 1979, **Horowitz** and Calvert, 1978; **Moortgat** et al., 1983). The present fit and the theoretical curve from **Troe** (2007) are given by full lines. Recommended data are represented by small symbols connected by a thin line: **JPL** (Sander et al., 2011); **IUPAC (2006)**, and **IUPAC (2013)**.



1  
2  
3  
4  
5  
6  
7  
8  
9

**Figure 4:** Spectra of the actinic photon flux density (WMO, 1985), the optical absorption cross section (Gratien et al., 2007) and  $\Phi_{\text{mol}}$  at 30 km altitude,  $33^\circ$  solar zenith angle, 227 K. The shaded area represents the integrand  $\sigma \cdot \Phi \cdot F_\lambda$  of Eq.(11).



1  
2

3 **Figure 6:** Comparison of the altitudinal profiles of the photolysis frequencies of  
 4 formaldehyde from **JPL** (Sander et al., 2011); **IUPAC (2006)**, **IUPAC (2013)**, and the  
 5 present work: total photolysis (a), molecular channel (b), and radical channel (c). The  
 6 frequencies are depicted for two solar zenith angles (SZA). The shaded areas mark the  $1\sigma$   
 7 error bounds of the profiles based on the errors of the fitting parameters for the present  
 8 quantum yields. (The arrows point to the related ordinate)

# 1 A simple formulation of the CH<sub>2</sub>O photolysis quantum yields

2

3 E.-P. Röth<sup>1</sup> and D. H. Ehhalt<sup>2</sup>

4 [1]{Institute for Energy and Climate Research (IEK-7: Stratosphere), Research Center Jülich,  
5 Germany }

6 [2]{Institute for Energy and Climate Research (IEK-8: Troposphere), Research Center Jülich,  
7 Germany }

8 Correspondence to: E.-P. Röth (e.p.roeth@fz-juelich.de)

9

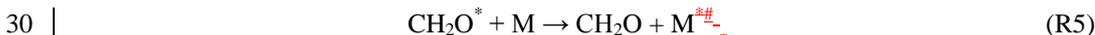
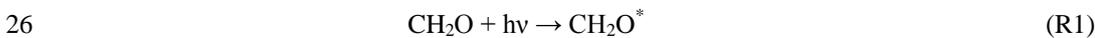
## 10 Abstract

11 New expressions for the ~~various-wavelength-wavelength~~-dependent photolysis quantum yields  
12 of CH<sub>2</sub>O,  $\Phi_j$ , are presented. They are based on combinations of functions of the type  
13  $A_i/(1+\exp[-(1/\lambda-1/\lambda_{0i})/b_i])^{-1}$ . The parameters  $A_i$ ,  $b_i$ , and  $\lambda_{0i}$  which have a physical meaning are  
14 obtained by fits to the measured data of the  $\Phi_j$  available from the literature. The altitude  
15 dependence of the photolysis frequencies resulting from the new quantum yield expressions  
16 are compared to those derived from the  $\Phi_j$  recommended by JPL and IUPAC.

17

## 18 1. Introduction

19 Formaldehyde, CH<sub>2</sub>O, is an important trace gas in the atmosphere. It is formed as an  
20 intermediate in the oxidation of methane and non-methane hydrocarbons, and destroyed by  
21 the reaction with OH and by photolysis in the near ultraviolet. The photolysis involves several  
22 channels. Following the excitation (R1), CH<sub>2</sub>O\* can decay into purely molecular products  
23 (R2), or into products that in the atmosphere lead to the eventual formation of hydroperoxy  
24 radicals, HO<sub>2</sub>, (R3, R4). The quenching reaction R5 and fluorescence R6 can influence the  
25 quantum yields of the product channels.



32 As it turns out the molecular channel, R2, provides the by far largest source of molecular  
33 hydrogen, H<sub>2</sub>, in the atmosphere (Ehhalt and Rohrer, 2009). The radical channels, R3 and R4,  
34 that generate HO<sub>2</sub> radicals, enhance local photochemistry. Finally each destruction of a CH<sub>2</sub>O



1 molecule – including that by OH – eventually results in a carbon monoxide molecule, CO. As  
2 a consequence CH<sub>2</sub>O is also an important source of CO in the atmosphere.

3 Recognizing the importance for atmospheric chemistry the quantum yields of the CH<sub>2</sub>O  
4 photolysis were measured early on and by various authors (see Sander et al., 2011, Atkinson  
5 et al., 2006, and the internet version IUPAC (2013) for summaries).

6 The quantum yield  $\Phi_{\text{mol}}$  of the molecular branch R2 was usually measured by monitoring the  
7 H<sub>2</sub> production while scavenging the H atoms to prevent their contribution to the H<sub>2</sub>  
8 production (e.g.: Moortgat et al., 1978, Horowitz and Calvert, 1978). The formation of the  
9 molecular products via the reaction path of a roaming H-atom [see e.g. Bowman and Shepler,  
10 2011 and Christoffel and Bowman, 2009] was not known then and is not included explicitly  
11 in our list of reactions but it is included in reaction R2, and its quantum yield is part of the  
12 measured  $\Phi_{\text{mol}}$ .

13 Reactions R3 and R4 form the radical channel with the combined quantum yield  $\Phi_{\text{rad}}$  which  
14 in some cases was investigated directly by measuring the products, H and CHO (e.g.: Smith et  
15 al., 2002, Gorrotxategi et al., 2008, Tatum Ernest et al., 2012).

16 The fluorescence quantum yield (R6) was measured by Miller and Lee, 1978, in the  
17 wavelength range 290 to 360 nm. Its maximum at 353 nm is less than 3.5 % and it is less than  
18 1% at the other wavelengths considered. It will, therefore, be neglected here. We know of no  
19 measurements below 290 nm.

20 The total quantum yield  $\Phi_{\text{tot}}$ , i.e. the fraction of the decay of excited formaldehyde, CH<sub>2</sub>O\*,  
21 into products other than its ground state, was derived from the CO production. By definition  
22  $\Phi_{\text{tot}}$  is the sum of the quantum yields of the molecular and the radical channel:

$$\Phi_{\text{tot}} = \Phi_{\text{mol}} + \Phi_{\text{rad}} \quad (1)$$

24 The measured wavelength dependences of the quantum yields are usually given in tabular  
25 form (see e.g. Atkinson et al., 2006, IUPAC, 2013). ~~For  $\Phi_{\text{rad}}$  also or as~~ a fit by a fourth order  
26 polynomial (see Sander et al., 2011) ~~exists~~. To provide a more handy tool for atmospheric  
27 modeling we propose to use ~~combinations-sums~~ of energy dependent functions of the type

$$\frac{A}{1 + \exp\left[\frac{-(1/\lambda - 1/\lambda_0)}{b}\right]} \quad (2)$$

29 to fit  $\Phi_{\text{mol}}$  and  $\Phi_{\text{rad}}$ . These functions are ~~well-well-~~suited to map smooth transitions. They  
30 allow to include pressure and temperature dependences. And the resulting parameters are few  
31 and have a physical meaning; in particular  $1/\lambda_0$  corresponds to the threshold energy of the  
32 respective reaction; b describes the width of the transitions. Moreover, the formalism should  
33 also provide a useful template for the formulation of the analogous  $\Phi_i$  for the isotopologues of

1 formaldehyde. In particular we hope to eventually construct expressions of the quantum yields  
2 for CHDO for which –apart from the threshold energies and a few isotope fractionation  
3 factors- no direct measurements exist.

4 Our analysis of the quantum yields will be based on the data filed by JPL (Sander et al., 2011)  
5 and IUPAC (2006) omitting all measurements ~~with an obvious bias whose wavelength~~  
6 dependencies deviate strongly from the forms recommended by JPL or IUPAC (e.g. McQuigg  
7 and Calvert, Clark et al., Tang et al. for  $\Phi_{\text{rad}}$ ). Likewise, ~~only publications of independent~~  
8 ~~measurements were taken into account, i.e.~~ if measured data appear in several publications by  
9 the same authors, only the latest data were considered. Not all data are independent of each  
10 other, as some measurements (Smith et al., 2002, Pope et al., 2005, Tatum Ernest et al., 2012)  
11 are relative and normalized to absolute quantum yields (DeMore et al., 1997, Sander et al.,  
12 2011). This influences the uncertainty range of the parameters  $A_i$  whose  $1\sigma$  errors might be  
13 somewhat larger than indicated in the respective equations.

Formatiert: Nicht Hervorheben

14 First, in Sections 2 to 4, we will fit the measured wavelength dependences of the various  $\Phi$   
15 separately and compare them to those reported in the literature. In a second step, after having  
16 convinced ourselves that the parameters from the separate fits that should correspond to each  
17 other are indeed similar in value, we attempt a simultaneous fit of all  $\Phi$  in ~~chapter~~Chapter 5.

## 19 2. The quantum yield of the radical channel

20 Most publications on the formaldehyde photolysis deal with the radical channel R3 - notably:  
21 Horowitz and Calvert (1978), Moortgat et al. (1983), Smith et al. (2002), Gorrotxategi et al.  
22 (2008), and Tatum Ernest et al. (2012). Nearly all of these measurements were made at room  
23 temperature, and experiments and theory indicate that there is no pressure dependence of  $\Phi_{\text{rad}}$ .  
24 We, therefore, assume all these data to be comparable and their variance attributable to  
25 experimental error. Thus all these data are combined in Figure 1 ~~without any weighing~~. Smith  
26 et al. (2002) attributed some of the variance in their data to a line structure in  $\Phi_{\text{rad}}$ . The  
27 possibility of a line structure appears corroborated by the data of Tatum Ernest et al. (2012),  
28 which show a strong feature in  $\Phi_{\text{rad}}$  at 321 nm. For comparison the data of Tatum Ernest et al.  
29 are also shown in Figure 1, but they are not used for the fit.

30 To fit the experimentally observed wavelength dependence of  $\Phi_{\text{rad}}$  we use a combination of  
31 two functions of the type mentioned above, one for the ~~long-wave~~ decay of  $\Phi_{\text{rad}}$  to longer  
32 wavelengths at about 328 nm, the other for the ~~short-wave~~ decay towards shorter wavelengths  
33 at 277 nm. To obtain the fit parameters and their errors a simplex algorithm (Nelder and

1 Mead, 1965) is used in combination with a bootstrapping method with 2000 arbitrary  
 2 removals of 20 % of the data. The result is given by Eq. (3), with  $\lambda$  in nm:

$$3 \quad \Phi_{rad} = \frac{0.72 \pm 0.01}{1 + \exp\left(\frac{-(1/\lambda - 1/328.0 \pm 0.6)}{(5.2 \pm 0.6) \cdot 10^{-5}}\right)} - \frac{0.38 \pm 0.03}{1 + \exp\left(\frac{-(1/\lambda - 1/278.4 \pm 0.8)}{(4.7 \pm 1.1) \cdot 10^{-5}}\right)} \quad (3)$$

4 ~~Eq. (3)~~ Equation 3 is also shown in Fig.1.

5 Eq. (3) holds primarily for room temperature. ~~Its first term defines the decay of  $\Phi_{rad}$  to longer~~  
 6 ~~wavelengths, its second term the decay towards shorter wavelengths.~~ The respective

7 parameters will be labelled by the subscripts l,s. The  $\lambda_0$  mark the inflection points in the

8 decays:  $\lambda_{0,l} = 328.0$  nm;  $\lambda_{0,s} = 278.4$  nm. The corresponding b define the wavelength interval

9 within which the decrease takes place. Owing to the scatter in the measured  $\Phi_{rad}$  data all

10 these parameters exhibit an uncertainty range. The estimated 1  $\sigma$  errors ~~are listed in Table 1~~

11 ~~along with the values of the parameters of the parameters are also entered in Equation 3.~~ We

12 note that  $\lambda_{0,l}$  closely corresponds to the dissociation energy of the H-CHO bond namely

13  $30328.5 \text{ cm}^{-1}$  or 329.7 nm (Terentis et al., 1998) and that  $\lambda_{0,s}$  approximately corresponds to

14 the heat of ~~formation-reaction~~ of ~~reaction~~-R4 namely 423 kJ/mol or 283 nm (Sander et al.,

15 2011).

16 Moortgat et al. (1983) have also measured the wavelength dependence of  $\Phi_{rad}$  at 220 K. Given

17 the experimental variance in those admittedly sparse data, Eq. (3) also fits the measured  $\Phi_{rad}$

18 at 220 K quite well (not shown here). Thus, as far as the experimental data on  $\Phi_{rad}$  are

19 concerned, Eq. (3) covers the temperature range of 220 K to 300 K relevant for atmospheric

20 modeling and there is no immediate need to introduce a temperature dependence. On the other

21 hand, theoretical considerations suggest the inclusion of the internal energy of the CH<sub>2</sub>O

22 molecule, and this can be easily done: Following Troe (2007) one can add a term 3kT

23 (appropriately scaled) to  $1/\lambda$  in the left hand term of Eq. (3). In Section ~~65, Discussion~~, we

24 will investigate the impact of this T dependence (see Eq. 12) on the altitude profile of the

25 respective photolysis frequency. In principle, another weak T dependence can arise through

26 the parameter b. That dependence could be easily accommodated by replacing b by  $(b_0 + b_1T)$

27 should future  $\Phi_{rad}$  measurements provide enough information to warrant such a step.

28 The present formulation of Eq. (3) with constant parameters b - i.e. b independent of  $\lambda$  -

29 forces the decrease to be nearly symmetrical around the respective  $\lambda_0$ . This is not necessarily

30 realistic. Again, if future measurements or theoretical considerations should prove the need,

31 an asymmetry could be easily accommodated by allowing b to depend on  $\lambda$ .

1 Finally, we note, that a line structure could be superimposed on Eq. (3) without difficulty. For  
2 the moment we refrain from doing so for two reasons: 1) As Tatum Ernest et al. (2012)  
3 ~~showed already indicated~~ even the strong feature in  $\Phi_{\text{rad}}$  at 321 nm ~~would produce only a~~  
4 ~~small change in~~ the photolysis frequencies in the atmosphere,  ~~$j_{\text{rad}}$~~ . ~~In fact superposition of~~  
5 ~~this feature on Equation 3 would increase  $j_{\text{mol}}$  by less than 2 % at all altitudes and decrease  $j_{\text{rad}}$~~   
6 ~~by less than, by only~~ 4%, because it coincides with a ~~strong small value~~ minimum in the  
7 absorption coefficient of  $\text{CH}_2\text{O}$ . Thus the error possibly introduced by its neglect is  
8 comparatively small (see discussion below). 2) The measurements of  $\Phi_{\text{rad}}$  by Smith et al.  
9 (2002), and Gorrotxategi et al. (2008) contain data points close to 321 nm which fall right on  
10 the average  $\Phi_{\text{rad}}$  given by Eq. (3). They were made with sufficient resolution to resolve the  
11 feature at 321 nm and are therefore somewhat at variance with the finding of Tatum Ernest et  
12 al. (2012).

13 Fig. 1 also contains the recommended wavelength dependences of  $\Phi_{\text{rad}}$  given in the  
14 evaluations by JPL (Sander et al., 2011), ~~and IUPAC (2006), and IUPAC (2013)~~. The reason  
15 for the ~~choice inclusion~~ of IUPAC (2006) ~~over IUPAC (2013)~~ is that ~~the former~~ ~~these~~ data,  
16 which were first published in 2002 and remained in the internet until 2012, had many users in  
17 the past and possibly still has at present. Further included is the theory-based dependence  
18 derived by Troe (2007); it covers only the restricted wavelength range from 310 to 350 nm.  
19 As a quantitative measure of the quality of these fits we ~~here~~ ~~add here~~ the coefficient of  
20 determination  $c$ . In the present case this is identical to the correlation coefficient between  
21 fitted and measured data. These correlation coefficients are:  $c = 0.821$  (IUPAC, 2006);  $c =$   
22  $0.840$  (Troe, 2007);  $c = 0.898$  (JPL, 2011);  ~~$c = 0.876$  (IUPAC, 2013)~~, and  $c = 0.905$  (this  
23 work); that is the quality of these various fits does not differ drastically.

24

### 25 3. The total quantum yield

26 There are more direct measurements for  $\Phi_{\text{tot}}$  and its dependence on  $\lambda$  than for  $\Phi_{\text{mol}}$ . To obtain  
27 higher accuracy we, therefore, first obtain a fit for  $\Phi_{\text{tot}}(\lambda)$  and then use Eq. (1), i.e.  $\Phi_{\text{mol}} = \Phi_{\text{tot}}$   
28  $- \Phi_{\text{rad}}$  for a fit of  $\Phi_{\text{mol}}(\lambda)$ . That fit is later compared to the measured dependence of  $\Phi_{\text{mol}}$  on  $\lambda$ .  
29 The available measurements of  $\Phi_{\text{tot}}(\lambda)$  at 300 K temperature and 1013 hPa pressure are  
30 reproduced in Figure 2. The values of  $\Phi_{\text{tot}}$  at 355 nm and 353 nm were obtained by  
31 interpolating the respective Stern-Volmer plots given by Moortgat et al. (1979, 1983) to the  
32 pressure of 1 atm. The  $\Phi_{\text{tot}}$  values at  $\lambda < 340$  nm are pressure independent. The measured  
33  $\Phi_{\text{tot}}(\lambda)$  exhibits three regions: a plateau between 290 and 330 nm, a steep decrease to zero at  
34 longer wavelengths, and a weak decrease to  $\Phi_{\text{tot}} \sim 0.8$  at shorter wavelengths. The average

1 measured  $\Phi_{tot}$  in the plateau is  $1.06 \pm 0.09$  – not significantly different from 1 – the maximum  
 2 possible value. Therefore, in the fit we will fix this value to unity. The separation of the two  
 3 decreases by a plateau with  $\Phi_{tot}=1$  also means that it is possible to fit these two regions of  
 4 decrease separately and independently of each other.

5 The measurements in Figure 1 indicate that  $\Phi_{rad}$  vanishes at  $\lambda > 340$  nm; at those wavelengths  
 6  $\Phi_{tot}$  becomes identical to  $\Phi_{mol}$ . Moreover, tunneling processes extend the photolysis of  $\text{CH}_2\text{O}$   
 7 to  $\text{H}_2$  and  $\text{CO}$  well beyond the threshold energy of about 350 nm (Troe, 2007). In this energy  
 8 regime the rate of decay into the molecular channel decreases to values where collisional  
 9 quenching of the excited formaldehyde molecule (R5) begins to compete. Consequently,  $\Phi_{mol}$   
 10 and  $\Phi_{tot}$  become pressure dependent. Based on theoretical modeling and comparison with the  
 11 data of Moortgat et al. (1978, 1983), Troe (2007) proposed a Stern-Volmer formulation for  
 12  $\Phi_{mol}$  for  $\lambda > 340$  nm:

$$13 \quad \Phi_{mol} = \frac{1}{1 + 1.4 \exp(c(\lambda - \lambda_0))(M/M_0)} \quad (4)$$

14 with  $\lambda_0 = 349$  nm;  $c = 0.225 \text{ nm}^{-1}$  for  $\lambda > \lambda_0$  and  $c = 0.205 \text{ nm}^{-1}$  for  $\lambda < \lambda_0$  and  $M$  the number  
 15 density of the bath gas.  $M_0 = 2.46 \times 10^{19} \text{ cm}^{-3}$ , the number density at 1013 hPa pressure and  
 16 300 K temperature. Troe (2007) also pointed out that on theoretical grounds the temperature  
 17 dependence of  $\Phi_{mol}$  should be small compared to the experimental uncertainties and thus  
 18 negligible at this stage. This is somewhat at variance to the measurements by Moortgat et al.  
 19 (1983) which seem to indicate such a dependency, albeit with large uncertainties.

20 Since  $\Phi_{tot}$  equals  $\Phi_{mol}$  for  $\lambda > 340$  nm where nearly all of the change in  $\Phi_{tot}$  with wavelength  
 21 is located, and since Eq. (4) approaches unity for  $\lambda < 330$  nm, Eq. (4) should also provide a  
 22 good approximation for  $\Phi_{tot}(\lambda)$ . In fact we could use it with its current parameters as our  
 23 intended fit (see Figure 2).

24 However, we prefer to formulate our fit in terms of energy, i.e.  $1/\lambda$ . Moreover, a direct fit to  
 25 the data in Figure 2 will merge the pre-exponential factor in Eq. (4) with  $\lambda_0$ . So, instead of  
 26 using Eq. (4) we will fit Eq. (5) to the data at  $\lambda > 310$  nm in Figure 2:

$$27 \quad \Phi_{tot} = \frac{1}{1 + \exp\left(\frac{-\left(\frac{1}{\lambda} - \frac{1}{\lambda_{0,l}}\right)}{b_l}\right) \cdot (M/M_0)} \quad (5)$$

28 Our fit yields the parameters  $\lambda_{0,l}$  and  $b_l$  of [Table 2 Eq. \(6\)](#). In this case  $\lambda_{0,l}$  has a somewhat  
 29 different meaning than before. Here,  $\lambda_{0,l}$  not only depends on the threshold energy of the  
 30 reaction involved, but also on the quenching efficiency with which energy is drained from the

excited CH<sub>2</sub>O molecule. But as before,  $\lambda_{0,1}$  represents the inflection point in the decrease of  $\Phi$ , at least for  $M = M_0$ .

The fit of  $\Phi_{tot}$  for the short wave decrease relies on our model Eq. (2) and yields the parameters listed in Table 2 adds the second term in Eq. (6) for  $\Phi_{tot}$ .

The equation for  $\Phi_{tot}(\lambda)$  over the full wavelength range therefore is:

$$\Phi_{tot} = \frac{1}{1 + \exp\left(\frac{-(1/\lambda - 1/347.1 \pm 0.7)}{(5.7 \pm 0.8) \times 10^{-5}}\right)} \left(M/M_0\right) - \frac{0.20 \pm 0.01}{1 + \exp\left(\frac{-(1/\lambda - 1/284.3 \pm 0.9)}{(3.5 \pm 1.4) \times 10^{-5}}\right)} \quad (6)$$

with  $\lambda$  given in nm.

We have not been able to find a ready explanation for the experimentally observed weak decrease of  $\Phi_{tot}$  at shorter wavelengths in the literature. We note, however, that  $\lambda_{0,s}=284.3$  corresponds closely to the heat of formation reaction for R4reaction (4) (see Section 2).

Following the arguments by Troe (2007) we assume the temperature dependence of  $\Phi_{tot}(\lambda)$  to be negligible. But here again, our fitting functions could readily be modified to include a T dependence.

$\Phi_{tot}(\lambda)$  from Eq. (6) is also shown in Figure 2. It compares favorably to the measured data of  $\Phi_{tot}$ . For additional comparison Figure 2 also contains the recommended wavelength dependences of  $\Phi_{tot}$  given in the evaluations by JPL (Sander et al., 2011), IUPAC (2013), and IUPAC (2006). Further included is the dependence derived from Troe's (2007)  $\Phi_{mol}$ ; it covers only the restricted wavelength range from 310 to 370 nm. Just as Eq. (6), the  $\Phi_{tot}(\lambda)$  from JPL and that based on Troe (2007) agree well with the measurements. An exception are the recommended values from IUPAC (2006) which clearly deviate from the measurements in the range  $330 \text{ nm} < \lambda < 350 \text{ nm}$ . As a consequence of this deviation on the coefficient of determination is ~~poor~~ relatively small:  $c = 0.898913$ , whereas the others are: JPL,  $c = 0.959$ ; Troe,  $c = 0.944$ ; present,  $c = 0.956$ . In IUPAC (2013) this deviation is removed; the corresponding  $c$  is 0.924.

#### 4. The quantum yield of the molecular channel

Since  $\Phi_{mol}$  is given by  $\Phi_{tot} - \Phi_{rad}$ , it could be simply obtained from the difference of Eqs. (6) and (3). Explicitly:

$$\Phi_{mol} = \Phi_{tot} - \Phi_{rad} = \frac{1}{1 + \exp\left(\frac{-(1/\lambda - 1/327.1)}{5.7 \times 10^{-5}}\right)} \left(\frac{M}{M_0}\right) - \frac{0.20}{1 + \exp\left(\frac{-(1/\lambda - 1/284.3)}{3.5 \times 10^{-5}}\right)} + \frac{0.72}{1 + \exp\left(\frac{-(1/\lambda - 1/328.0)}{5.2 \times 10^{-5}}\right)} + \frac{0.38}{1 + \exp\left(\frac{-(1/\lambda - 1/278.4)}{4.7 \times 10^{-5}}\right)} \quad (7)$$

On the other hand,  $\Phi_{mol}$  can be obtained by a direct fit to the measured data. This requires a combination of only three functions of the Eq.(2) type and the fit results in:

$$\Phi_{mol} = \frac{1}{1 + \exp\left(\frac{-(1/\lambda - 1/345.2 \pm 0.8)}{(6.2 \pm 1.7) \times 10^{-5}}\right)} \left(\frac{M}{M_0}\right) - \frac{0.75 \pm 0.03}{1 + \exp\left(\frac{-(1/\lambda - 1/325.3 \pm 0.6)}{(3.9 \pm 0.5) \times 10^{-5}}\right)} + \frac{0.24 \pm 0.05}{1 + \exp\left(\frac{-(1/\lambda - 1/274.2 \pm 3.3)}{(2.3 \pm 2.1) \cdot 10^{-5}}\right)} \quad (87)$$

Eq. (87) makes the implicit assumption that the short wave decreases in  $\Phi_{tot}$  and  $\Phi_{rad}$  (second and fourth term in Eq. (7)) have the same  $\lambda_{0,s}$  and  $b_s$ . The estimated  $1\sigma$  errors along with of the fit parameters are listed in Table 3 entered in Eq. (7).

In Figure 3  $\Phi_{mol}(\lambda)$  from Eq. (87) is compared to the measured data on  $\Phi_{mol}(\lambda)$ . The latter consist of direct measurements of  $\Phi_{mol}$  by Moortgat et al. (1979; 1983), and data based on measured  $\Phi_{tot}$  and  $\Phi_{rad}$  by Horowitz and Calvert (1978). The agreement of Eq. (87) with the measurements is quite reasonable. For further comparison Figure 3 also includes the recommendations by JPL (Sander et al., 2011), IUPAC (2013), and IUPAC (2006) as well as a fit based on  $\Phi_{tot}$  and  $\Phi_{rad}$  derived from Troe (2007). The respective coefficients of determination are:  $c = 0.822$  (IUPAC, 2006);  $c = 0.838$  (Troe, 2007);  $c = 0.947$  (JPL; 2011);  $c = 0.843$  (IUPAC, 2013);  $c = 0.958$  (this work); IUPAC (2013) would yield  $c = 0.843$ .

## 5. Simultaneous fit of $\Phi_{rad}$ , $\Phi_{mol}$ , and $\Phi_{tot}$

A comparison of the parameters and their errors obtained from the individual fits of the various  $\Phi$  suggests that the  $\lambda_{0,s}$ ,  $\lambda_{0,m}$ ,  $\lambda_{0,l}$  and  $b_s$ ,  $b_m$ ,  $b_l$  in a given fit equation do not differ significantly from the corresponding parameters in the others. We felt, therefore, felt justified to attempt a simultaneous fit of all  $\Phi$ . In this attempt we assume that the corresponding  $\lambda_0$  and  $b$  parameters in the various equations for  $\Phi$  are indeed identical. We further assume that  $\Phi_{tot}$  reaches a maximum value of 1 and that Eq. (1) holds. With these assumptions the total number of fit parameters for all three  $\Phi$  together reduces to 9. The simultaneous calculation of the 9 unknown parameters results in the equations for the  $\Phi_i$  listed in Table 4-1, The

1 ~~coefficients of determination their estimated 1  $\sigma$  errors are also entered in the~~  
2 ~~equation together with the function parameters and their estimated 1  $\sigma$  errors are tabulated in~~  
3 ~~Table 5.~~

4 The functions of Table 4-1 differ somewhat, but hardly significantly from those given by Eqs.  
5 (3), (6) and (87) considering the experimental uncertainties. The coefficients of determination  
6 are comparable to those from the individual fits: ~~c=0.904 for  $\Phi_{\text{rad}}$ , 0.951 for  $\Phi_{\text{tot}}$ , and 0.934 for~~  
7  ~~$\Phi_{\text{mol}}$ . The relative errors of the parameters of  $\Phi_{\text{tot}}$  of the shortwave decay are identical to~~  
8 ~~those of  $\Phi_{\text{rad}}$  by definition, as it is the case for the errors of the  $\Phi_{\text{mol}}$  function.~~ Because of  
9 their simplicity Eqs. (9), (108), and (110) represent our preferred formulation of the CH<sub>2</sub>O  
10 quantum yields and will be used in the discussion below.

## 11 12 **6. Discussion**

13 In the foregoing sections we presented new formulations of  $\Phi_{\text{tot}}$ ,  $\Phi_{\text{rad}}$ , and  $\Phi_{\text{mol}}$  for CH<sub>2</sub>O. The  
14 presentation also made it ~~also~~ clear that there is room for improvements. One concerns the  
15 temperature dependence of  $\Phi$ . Given the experimental uncertainties we have refrained from  
16 providing T dependences for the  $\Phi$ 's. But there are temperature dependences in the literature,  
17 which could be incorporated in our formulation (Atkinson et al., 2006; Troe, 2007; Sander et  
18 al., 2011). Below we will incorporate such a temperature dependence in  $\Phi_{\text{rad}}$  to test the  
19 sensitivity of the corresponding photolysis frequencies of CH<sub>2</sub>O to the vertical temperature  
20 profile.

21 In addition the question of line structure in  $\Phi_{\text{rad}}$  needs eventually to be resolved.

22 Of major interest to the atmospheric chemist is the impact of this new formulation of  $\Phi$  on the  
23 atmospheric photolysis frequencies of CH<sub>2</sub>O. That photolysis frequency  $j$  is given by:

$$24 \quad j = \int_0^{\infty} \Phi(\lambda) \sigma(\lambda) F_{\lambda}(\lambda) d\lambda \quad (121)$$

25 i.e. it also depends on the absorption cross-section,  $\sigma(\lambda)$ , of CH<sub>2</sub>O, and the local actinic  
26 photon flux density  $F_{\lambda}(\lambda)$ . For our calculations of  $j$  we will use the absorption spectrum  
27 measured by Gratien et al. (2007). It is, by the way, also slightly temperature dependent; the  
28 respective function can be found in Röth et al. (1997). Its effect on the  $j$  is quite small – e.g.  
29 less than 0.3 % for  $j_{\text{rad}}$  – and included in the calculations. The atmospheric actinic photon flux  
30 density consists of down-welling and up-welling contributions, and depends of course on the  
31 solar zenith angle and altitude. It was calculated by the radiative transfer program ART (Röth,  
32 2002) using the extraterrestrial solar flux from WMO (1985). All three factors under the  
33 integral strongly vary with wavelength,  $\lambda$ . (To various degrees they also vary with altitude.)



1 As an example Figure 4 shows  $\sigma(\lambda)$ ,  $F_\lambda(\lambda)$ , and  $\Phi_{\text{mol}}(\lambda)$ , together with the wavelength  
2 dependent integrand of Eq.(11) at 30 km altitude and  $33^\circ$  solar zenith angle. We particularly  
3 notice the sharp cutoff in  $F_\lambda(\lambda)$  around  $\lambda = 320$  nm caused by the absorption of solar UV in  
4 the ozone layer at lower wavelengths. This means that below 30 km altitude the exact form of  
5 the  $\Phi_i$  at  $\lambda < 300$  nm has little influence on the various photolysis frequencies. Figure 4  
6 further indicates how much the long-wave decrease of  $\Phi_{\text{mol}}$  is shifted towards longer  
7 wavelengths at the air density at 30 km altitude. In fact, this shift is so large that the long-  
8 wave cutoff of the integrand in Eq. ~~(11)~~ is no longer determined by  $\Phi_{\text{mol}}$ , as it is at low  
9 altitudes, but rather by the absorption spectrum of  $\text{CH}_2\text{O}$ . Hence, at altitudes above 30 km the  
10 exact form of the decrease in  $\Phi_{\text{mol}}$  and  $\Phi_{\text{tot}}$  at the longer wavelengths has no influence on the  
11 respective photolysis frequencies. The curve for  $\sigma \cdot F_\lambda$  in Fig.4 nicely illustrates why the line  
12 structure observed by Tatum Ernest et al. (2012) at 321 nm has so little impact on  $j_{\text{mol}}$ : It  
13 would increase the quite small feature at 321 nm in that product by only a factor of 1.5.  
14 Given the  $\Phi_i$  from the Eqs. (89) to ~~(10)~~ in Table 1,  $\sigma(\lambda)$  from Gratien et al. (2007) along  
15 with vertical temperature and density profiles of the U.S. standard atmosphere (NOAA, 1976)  
16 we can calculate the vertical profiles of the photolysis rates. They are shown in Figure 5  
17 calculations were made with 1 nm spectral resolution and are shown in Figure 5. The shaded  
18 areas mark the  $1\sigma$  error bounds of the  $j_i$  profiles based on the errors of the fitting parameters  
19 for  $\Phi_i$  given in Section 5. As to be expected, all  $j_i$  increase with altitude. In the case of  $j_{\text{rad}}$  that  
20 increase is essentially due to the vertical change in  $F_\lambda(\lambda)$ , since our  $\Phi_{\text{rad}}$  is neither temperature  
21 nor pressure dependent and thus independent of altitude, and the slight temperature  
22 dependence of  $\sigma(\lambda)$  makes a minor contribution only.  $j_{\text{tot}}$  and  $j_{\text{mol}}$ , however, are significantly  
23 modified by the density dependence in  $\Phi_{\text{mol}}$ .

Formatiert: Tiefgestellt

24 In Figure 5 we also demonstrate the impact of a possible temperature dependence in  $\Phi_{\text{rad}}$ . The  
25 temperature dependence is introduced by adding the term  $(300-T)(3k/hc)$  in the appropriate  
26 dimensional units to  $1/\lambda$  in the first term of Eq. (3) (see Troe, 2007, and Section 2.).

$$27 \quad \Phi_{\text{rad}} = \frac{0.74}{1 + \exp\left(\frac{-\left(\frac{1}{\lambda} + (300-T)\left(\frac{3k}{hc}\right) - \frac{1}{327.4}\right)}{5.4 \cdot 10^{-5}}\right)} - \frac{0.40}{1 + \exp\left(\frac{-\left(\frac{1}{\lambda} - \frac{1}{279.0}\right)}{5.2 \cdot 10^{-5}}\right)}$$

28 | (4312)

29 That means: Only the long-wave decay in  $\Phi_{\text{rad}}$  is considered to be temperature dependent.  
30 Here  $k$  is the Boltzmann constant,  $h$  the Planck constant, and  $c$  the speed of light. As Figure 5  
31 shows, a temperature dependence of this size clearly has a significant impact on  $j_{\text{rad}}$  and by  
32 virtue of  $\Phi_{\text{mol}} = \Phi_{\text{tot}} - \Phi_{\text{rad}}$  also on  $j_{\text{mol}}$ . The effect is largest at around 15 km, the height of the

1 temperature minimum, and about -9% for  $j_{\text{rad}}$ , respectively ca. +6% for  $j_{\text{mol}}$ . The temperature  
2 at 15 km is 220 K, i.e. the temperature shifts in  $j_{\text{rad}}$  and  $j_{\text{mol}}$  correspond to a temperature  
3 difference of 80 K. Apparently a correct formulation of the T-dependence of  $\Phi_{\text{rad}}$  could lead  
4 to a significant improvement in the predicted vertical profiles of  $j_{\text{rad}}$  and  $j_{\text{mol}}$ .  
5  $j_{\text{tot}}$  remains unaffected by the proposed temperature dependency. In fact, even assuming a  
6 temperature dependence of the kind above for the long-wave decay of  $\Phi_{\text{tot}}$  would have  
7 comparatively little impact on the  $j_{\text{tot}}$  profile. It would be masked by the air density  
8 dependence of  $\Phi_{\text{tot}}$ : Just as at lower densities, the exact form of the long-wave decay in  $\Phi_{\text{tot}}$   
9 no longer influences  $j_{\text{tot}}$ , so can its temperature dependence no longer influence  $j_{\text{tot}}$ .  
10 Finally, in Figure 6, we compare the photolysis frequencies based on this work's quantum  
11 yields to those calculated with the quantum yields recommended by IUPAC (2006), [IUPAC](#)  
12 [\(2013\)](#), and JPL (Sander et al., 2011). The JPL recommendation includes an explicit  
13 temperature dependence for  $\Phi_{\text{rad}}$ . In addition, both, JPL and IUPAC (2006), treat the density  
14 dependence of  $\Phi_{\text{mol}}$  in terms of atmospheric pressure, which introduces a further temperature  
15 dependence. Both temperature effects are included in the calculation of the respective  $j_i$   
16 profiles. The comparison demonstrates that even at present – without a representation of the  
17 temperature dependence - our  $\Phi_i$  provide vertical profiles of the photolysis frequency which  
18 agree well with those based on  $\Phi_i$  from the JPL recommendation - for all  $j_i$  and both solar  
19 zenith angles considered. The comparison with the data from Atkinson et al. (2006) is less  
20 favorable, especially for  $j_{\text{mol}}$ . This reflects the differences between  $\Phi_{\text{mol}}(\lambda)$  given here and  
21 that recommended by JPL on the one hand to that recommended by Atkinson et al. (2006) on  
22 the other, which were already apparent in Figures 2 and 3. The new quantum yields  
23 recommended by IUPAC in 2013 give photolysis rates which lie slightly ~~above~~below our  
24 ~~values~~curves for  $j_{\text{mol}}$ , just outside the error bounds.  
25 Although the derived  $j_i$  profiles as well as the fits to the measured  $\Phi_i$  (Figures 1 to 3) based on  
26 the JPL recommendation and on the present work appear reasonably equivalent, we feel ~~our~~  
27 formalism to be advantageous: Since it consistently formulates the wavelength dependence of  
28  $\Phi_i$  in terms of  $1/\lambda$ , its fitting parameters are in units of energy, and represent, or are close to,  
29 molecular parameters, notably threshold energies, which are often available and can serve as  
30 guides. Moreover, the formulation in units of energy makes it easy to introduce temperature  
31 dependences should future measurements or theoretical considerations demand it. For the  
32 same reasons our formalism should provide a useful template for the formulation of the  $\Phi_i$  for  
33 the isotopologues of formaldehyde and likewise for the photolysis quantum yields of many  
34 other molecules.

1  
2 [The article processing charges for this open-access publication have been covered by a](#)  
3 [Research Centre of the Helmholtz Association.](#)

#### 5 **References**

6 Atkinson, R., Baulch, D. L., Cox, R. A., Crowley, J. N., Hampson, R. F., Hynes, R. G.,  
7 Jenkin, M. E., Rossi, M. F., and Troe, J.: Evaluated kinetic and photochemical data for  
8 atmospheric chemistry: Volume II – gas phase reactions of organic species, *Atmos. Chem.*  
9 *Phys.*, 6, 3625 – 4055, 2006

10 Bowman, J. M. and Shepler, B. C.: Roaming Radicals, *Ann. Rev. Phys. Chem.*, 62, 531 –  
11 553, 2011

12 Christoffel, K. M. and Bowman, J. M.: Three Reaction Pathways in the  $H + HCO \rightarrow H_2 + CO$   
13 Reaction, *J. Phys. Chem. A*, 113, 4138 – 4144, 2009

14 [Clark, J. H., Moore, C. B., and Nogar, N. S.: The photochemistry of formaldehyde: Absolute](#)  
15 [quantum yields, radical reactions, and NO reactions, \*J. Chem. Phys.\*, 68, 1264 - 1271, 1978](#)

16 [DeMore, W. B., Sander, S. P., Howard, C. J., Ravishankara, A. R., Golden, D. M., Kolb, C.](#)  
17 [E., Hampson, R. F., Kurylo, M. J., Molina, M. J.: NASA panel for data evaluation, chemical](#)  
18 [kinetics and photochemical data evaluation for use in stratospheric modeling, JPL Publication](#)  
19 [97-4, 1997](#)

20 Gorrotxategi Carbajo, P., Smith, S. C., Holloway, A., Smith, C. A., Pope, F. D.,  
21 Shallcross, D. E., and Orr-Ewing, A. J.: Ultraviolet photolysis of HCHO: Absolute HCO  
22 quantum yields by direct detection of the HCO Radical photoproduct, *J. Phys. Chem. A*, 112,  
23 12437 – 12448, 2008

24 Gratien, A., [Piequet-Varrault, B., Orphal, J., Perrandin, E., Doussin, J.-F., and Flaud, J.-M.:](#)  
25 [Laboratory intercomparison of the formaldehyde absorption cross sections in the infrared](#)  
26 [\(1660–1820  \$\text{cm}^{-1}\$ \) and ultraviolet \(300–360 nm\) spectral region, \*J. Geophys. Res.\*, 112,](#)  
27 [D05305, doi:10.1029/2006JD007201](#) Nilsson, E., Doussin, J.-F., Johnson, M. S., Nielsen, C.  
28 J., Stenstrom, Y., and Picquet-Varrault, B.: UV and IR absorption cross-sections of HCHO,  
29 [HCDO, and DCDO, \*J. Phys. Chem. A\*, 111, 11506 - 11513, 2007](#)

30 Horowitz, A. and Calvert, J. [EG](#): Wavelength dependence of the quantum efficiencies of the  
31 primary processes in formaldehyde photolysis at 25°C. *Int. J. Chem. Kinetics*, 10, 805 – 819,  
32 1978

33 IUPAC (2006) : see Atkinson et al. (2006)

34 IUPAC (2013): IUPAC Task Group on Atmospheric Chemical Kinetic Data Evaluation –  
35 Data Sheet P1, <http://iupac.pole-ether.fr>, (last access: 16 January 2015) 2013

1 [McQuigg, R. D. and Calvert, J. G.: The photodecomposition of CH<sub>2</sub>O, CD<sub>2</sub>O, CHDO, and](#)  
2 [CH<sub>2</sub>O-CD<sub>2</sub>O mixtures at Xenon flash lamp intensities, J. Am. Chem. Soc., 91, 1590 – 1599,](#)  
3 [1969](#)

4 Miller, R. G. and Lee, E. K. C.: Single vibronic level photochemistry of formaldehyde in the  
5 A<sup>1</sup>A<sub>2</sub> state: Radiative and non radiative processes in H<sub>2</sub>CO, HDCO, and D<sub>2</sub>O, J. Chem. Phys.,  
6 68, 4448 – 4464, 1978

7 Moortgat, G. K., Slemr, F., Seiler, W., and Warneck, P.: Photolysis of formaldehyde: Relative  
8 quantum yields of H<sub>2</sub> and CO in the wavelength range 270 -360 nm, Chem. Phys. Letters, 54,  
9 444 – 447, 1978

10 Moortgat, G. K. and Warneck, P.: CO and H<sub>2</sub> quantum yields in the photodecomposition of  
11 formaldehyde in air, J. Chem. Phys., 70, 3639 – 3651, 1979

12 Moortgat, G. K., Seiler, W., and Warneck, P.: Photodissociation of HCHO in air: CO and H<sub>2</sub>  
13 quantum yields at 220 K and 300 K, J. Chem. Phys., 78, 1185 – 1190, 1983

14 Nelder, J. A. and Mead, R.: A simplex method for function minimization, Computer Journal,  
15 7, 308 -313, 1965

16 NOAA,; U.S. Standard Atmosphere, NOAA-S/T76-1562, [Washington D.C.](#),1976

17 Röth, E.-P.: Description of the anisotropic radiation transfer model ART to determine  
18 photodissociation coefficients, Ber. Forschungszentrum Jülich, Jül-3960, [Jülich](#),2002

19 Röth, E.-P., Ruhnke, R., Moortgat, G., Meller, R., and Schneider, W.: UV/VIS [Absorption](#)  
20 [absorption Cross-sections](#) and [Quantum Yields](#) for [Use](#) in  
21 [Photochemistry](#) and [Atmospheric Modeling](#). Part 2:  
22 Organic [Substances](#), Ber. Forschungszentrum Jülich, Jül-3341, [Jülich](#),1997

23 Sander, S. P., Friedl, R.R., Abbatt, J. P. D., Barker, J. R., Burkholder, J. B., Golden, D. M.,  
24 Kolb, C. E., Kurylo, M. J., Moortgat, G. K., Wine, P. H., Huie, R. E., and Orkin, V. L.:  
25 Chemical kinetics and photochemical data for use in atmospheric studies. Evaluation number  
26 17, JPL-Publication 10-6, [Pasadena](#),2011

27 Smith, G. D., Molina, L. T., and Molina, ~~NM~~. J.: Measurement of radical quantum yields [for](#)  
28 [from](#) formaldehyde photolysis between 269 and 339 nm, J. Phys. Chem. A, 106, 1233 – 1240,  
29 2002

30 [Tang, K. Y., Fairchild, P. W., and Lee, E. K. C.: Laser-induced photodecomposition of](#)  
31 [formaldehyde \(A<sup>1</sup>A<sub>2</sub>\) from its single vibronic levels. Determination of the quantum yield of H](#)  
32 [atom by HNO\\* \(A<sup>1</sup>A<sub>2</sub>\) chemiluminescence, J. Phys. Chem., 83, 569 – 573, 1979](#)

33 Tatum Ernest, C., Bauer, D., and Hynes, A. J.: Radical Quantum Yields from Formaldehyde  
34 Photolysis in the 30 300 – 32 890 cm<sup>-1</sup> (304 – 329 nm) Spectral Region: Detection of Radical

- 1 Products Using Pulsed Laser Photolysis – Pulsed Laser Induced Fluorescence, J. Phys. Chem.
- 2 A, 116, 6983 – 6995, 2012
- 3 Terentis, A. C., Waugh, S. E., Metha, G. F., and Kable, S. H.: HCO (N,K<sub>a</sub>,K<sub>c</sub>,J) distributions
- 4 from near-threshold photolysis of H<sub>2</sub>CO (J,K<sub>a</sub>,K<sub>c</sub>), J. Chem. Phys. 108, 3187 – 3198, 1998
- 5 Troe, J.: Analysis of quantum yields for the photolysis of formaldehyde at  $\lambda > 310$  nm, J.
- 6 Phys. Chem. A, 111, 3868 – 3874, 2007
- 7 | WMO: Atmospheric Ozone 1985, Vol. 1, WNO Report 16, [Genf](#), 1985
- 8

1  
 2 **Table 1:** Coefficients of the quantum yield function for the radical channel and 1- $\sigma$  errors of  
 3 Eq. 3.  
 4

coefficient	value	error
$A_1$	0.72	$\pm 0.01$
$\lambda_{0,1}$	328.0 nm	$\pm 0.6$ nm
$b_1$	$5.2 \times 10^{-5} \text{ nm}^{-1}$	$\pm 0.6 \times 10^{-5} \text{ nm}^{-1}$
$A_s$	0.38	$\pm 0.03$
$\lambda_{0,s}$	278.4 nm	$\pm 0.8$ nm
$b_s$	$4.7 \times 10^{-5} \text{ nm}^{-1}$	$\pm 1.1 \times 10^{-5} \text{ nm}^{-1}$

5  
 6

1  
2  
3  
4  
5

**Table 2:** Coefficients of the total quantum yield function and 1- $\sigma$  errors of Eq. 6.

<b>coefficient</b>	<b>value</b>	<b>error</b>
$A_l$	1.0	fixed
$\lambda_{0,l}$	347.1 nm	$\pm 0.7$ nm
$b_l$	$5.7 \times 10^{-5} \text{ nm}^{-1}$	$\pm 0.8 \times 10^{-5} \text{ nm}^{-1}$
$A_s$	0.20	$\pm 0.01$
$\lambda_{0,s}$	284.3 nm	$\pm 0.9$ nm
$b_s$	$3.5 \times 10^{-5} \text{ nm}^{-1}$	$\pm 1.4 \times 10^{-5} \text{ nm}^{-1}$

1  
2 **Table 3:** Coefficients of the quantum yield function for the molecular channel and 1- $\sigma$  errors  
3 of Eq. 8.  
4

coefficient	value	error
$A_l$	1.0	fixed
$\lambda_{0,l}$	345.2 nm	$\pm 0.8$ nm
$b_l$	$6.2 \times 10^{-5} \text{ nm}^{-1}$	$\pm 1.7 \times 10^{-5} \text{ nm}^{-1}$
$A_m$	0.75	$\pm 0.03$
$\lambda_{0,m}$	325.3 nm	$\pm 0.6$ nm
$b_m$	$3.9 \times 10^{-5} \text{ nm}^{-1}$	$\pm 0.5 \times 10^{-5} \text{ nm}^{-1}$
$A_s$	0.24	$\pm 0.05$
$\lambda_{0,s}$	274.2 nm	$\pm 3.3$ nm
$b_s$	$2.3 \times 10^{-5} \text{ nm}^{-1}$	$\pm 2.1 \times 10^{-5} \text{ nm}^{-1}$

5  
6



1  
2 | **Table 41:** Recommended quantum yield functions for use in atmospheric chemistry models  
3 (wavelength  $\lambda$  in nm).  
4

$$\Phi_{rad} = \frac{0.74 \pm 0.01}{1 + \exp\left(\frac{-(1/\lambda - 1/327.4 \pm 0.5)}{(5.4 \pm 0.5) \cdot 10^{-5}}\right)} - \frac{0.40 \pm 0.04}{1 + \exp\left(\frac{-(1/\lambda - 1/279.0 \pm 1.3)}{(5.2 \pm 2.4) \cdot 10^{-5}}\right)} \quad (98)$$

$$\Phi_{tot} = \frac{1}{1 + \exp\left(\frac{-(1/\lambda - 1/346.9 \pm 0.5)}{(5.4 \pm 0.3) \times 10^{-5}}\right)} (M/M_0) - \frac{0.22 \pm 0.02}{1 + \exp\left(\frac{-(1/\lambda - 1/279.0 \pm 1.3)}{(5.2 \pm 2.4) \times 10^{-5}}\right)} \quad (109)$$

$$\Phi_{mol} = \frac{1}{1 + \exp\left(\frac{-(1/\lambda - 1/346.9 \pm 0.5)}{(5.4 \pm 0.3) \times 10^{-5}}\right)} (M/M_0) - \frac{0.74 \pm 0.01}{1 + \exp\left(\frac{-(1/\lambda - 1/327.4 \pm 0.5)}{(5.4 \pm 0.5) \cdot 10^{-5}}\right)} + \frac{0.18 \pm 0.02}{1 + \exp\left(\frac{-(1/\lambda - 1/279.0 \pm 1.3)}{(5.2 \pm 2.4) \cdot 10^{-5}}\right)} \quad (110)$$

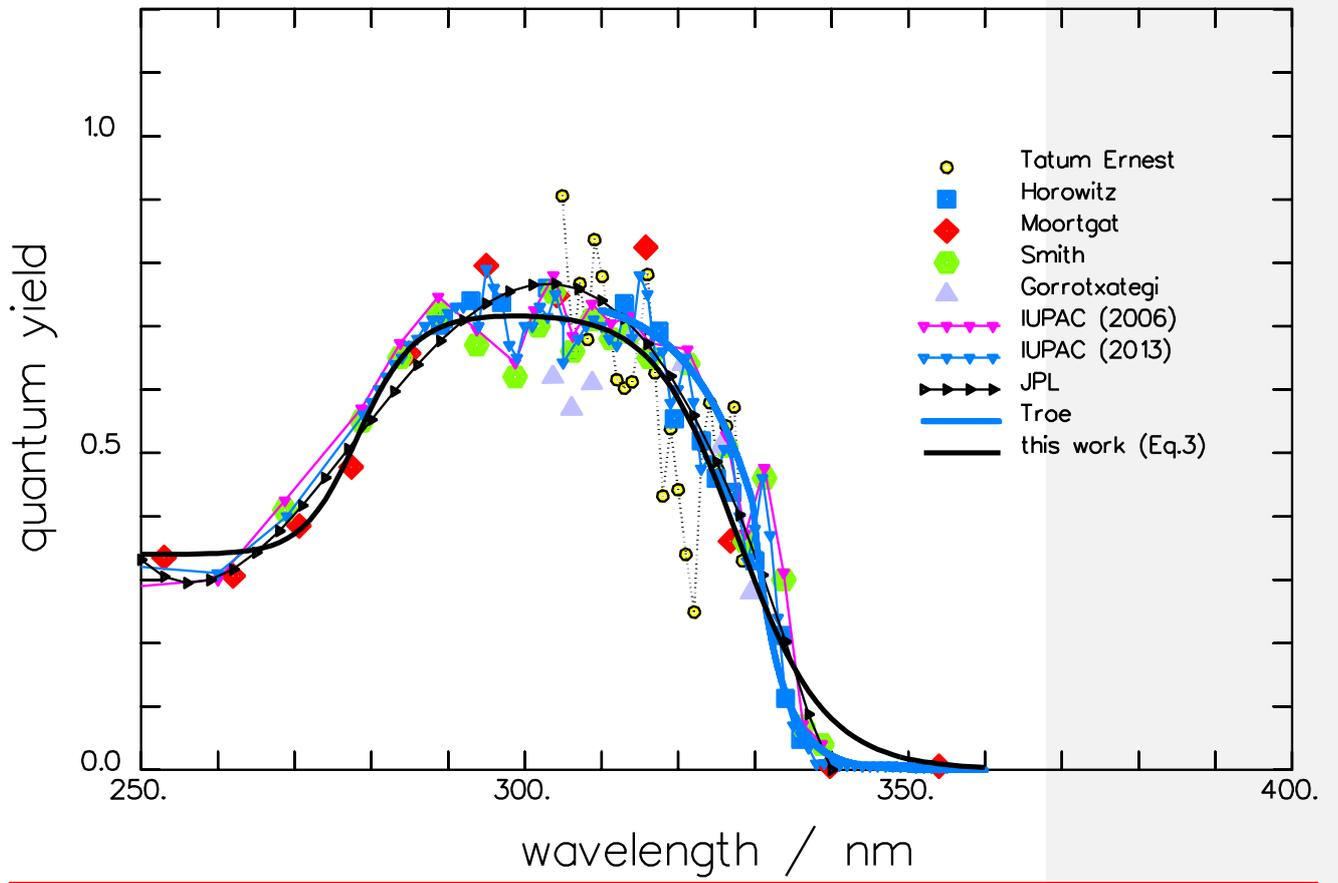
5  
6  
7

1  
2  
3  
4  
5

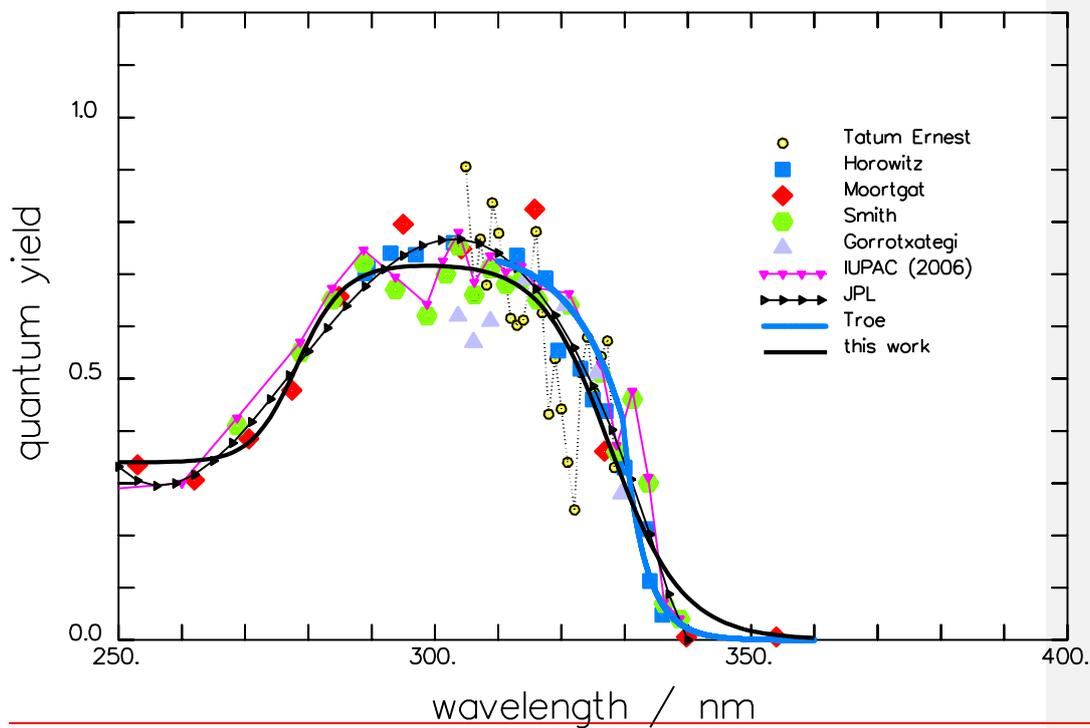
**Table 5:** Coefficients and 1  $\sigma$  errors of the equations in Table 4, along with the coefficients of determination  $e$  for the quantum yield functions. These parameters result from a global fit of all data, as described in Section 5.

	coefficient	value	error
	$A_i$	0.74	$\pm 0.01$
$\Phi_{\text{rad}}$ $e=0.904$	$\lambda_{0,i}$	327.4 nm	$\pm 0.5$ nm
	$b_i$	$5.4 \times 10^{-5} \text{ nm}^{-1}$	$\pm 0.5 \times 10^{-5} \text{ nm}^{-1}$
	$A_s$	0.40	$\pm 0.04$
	$\lambda_{0,s}$	279.0 nm	$\pm 1.3$ nm
	$b_s$	$5.2 \times 10^{-5} \text{ nm}^{-1}$	$\pm 2.4 \times 10^{-5} \text{ nm}^{-1}$
	$A_i$	1.0	fixed
$\Phi_{\text{tot}}$ $e=0.951$	$\lambda_{0,i}$	346.9 nm	$\pm 0.5$ nm
	$b_i$	$5.4 \times 10^{-5} \text{ nm}^{-1}$	$\pm 0.3 \times 10^{-5} \text{ nm}^{-1}$
	$A_s$	0.22	$\pm 0.02$
	$\lambda_{0,s}$	279.0 nm	$\pm 1.3$ nm
	$b_s$	$5.2 \times 10^{-5} \text{ nm}^{-1}$	$\pm 2.4 \times 10^{-5} \text{ nm}^{-1}$
	$A_i$	1.0	fixed
$\Phi_{\text{mol}}$ $e=0.934$	$\lambda_{0,i}$	346.9 nm	$\pm 0.5$ nm
	$b_i$	$5.4 \times 10^{-5} \text{ nm}^{-1}$	$\pm 0.3 \times 10^{-5} \text{ nm}^{-1}$
	$A_m$	0.74	$\pm 0.01$
	$\lambda_{0,m}$	327.4 nm	$\pm 0.5$ nm
	$b_m$	$5.4 \times 10^{-5} \text{ nm}^{-1}$	$\pm 0.5 \times 10^{-5} \text{ nm}^{-1}$
	$A_s$	0.18	$\pm 0.02$
	$\lambda_{0,s}$	279.0 nm	$\pm 1.3$ nm
	$b_s$	$5.2 \times 10^{-5} \text{ nm}^{-1}$	$\pm 2.4 \times 10^{-5} \text{ nm}^{-1}$

6



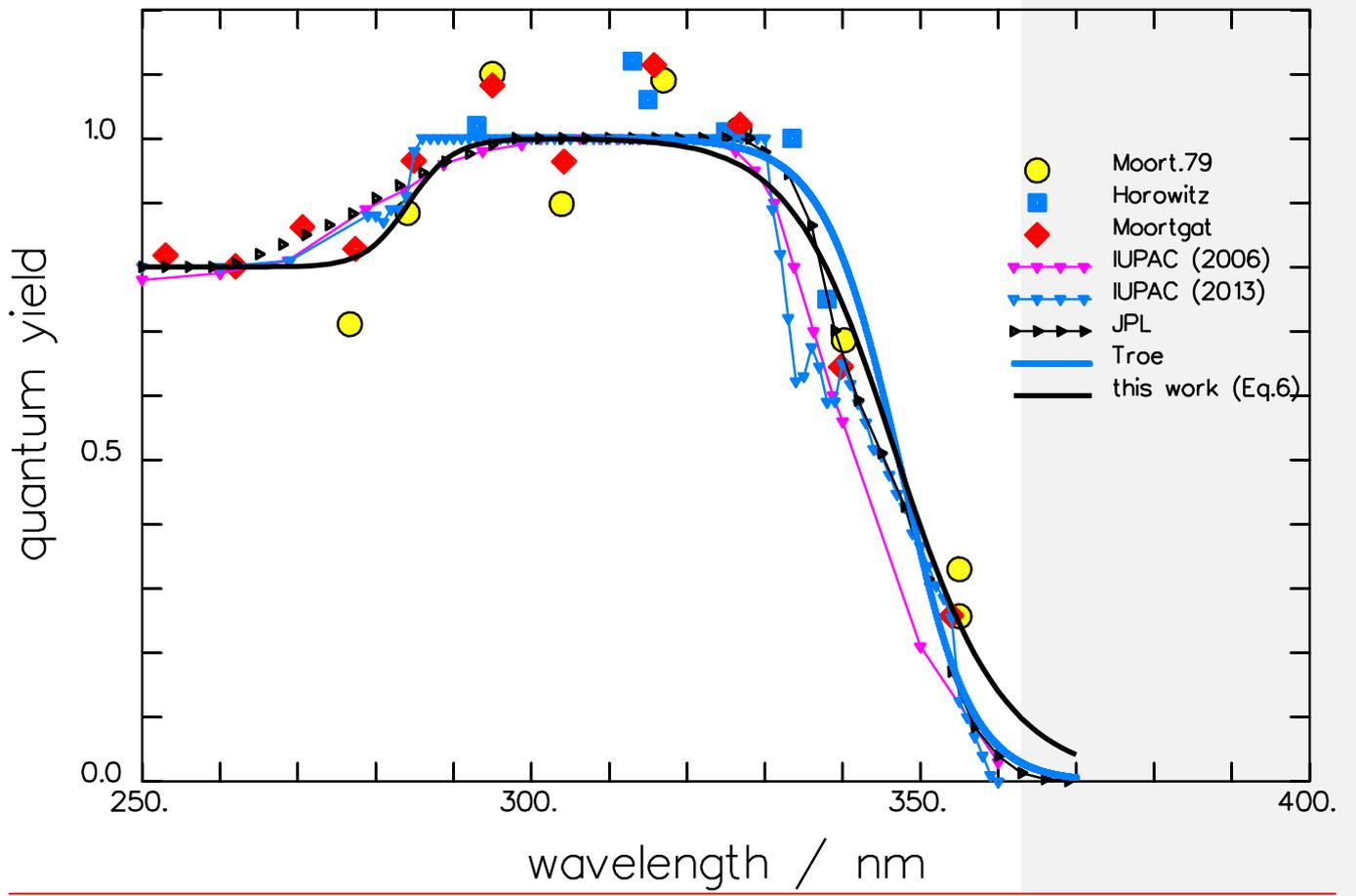
1



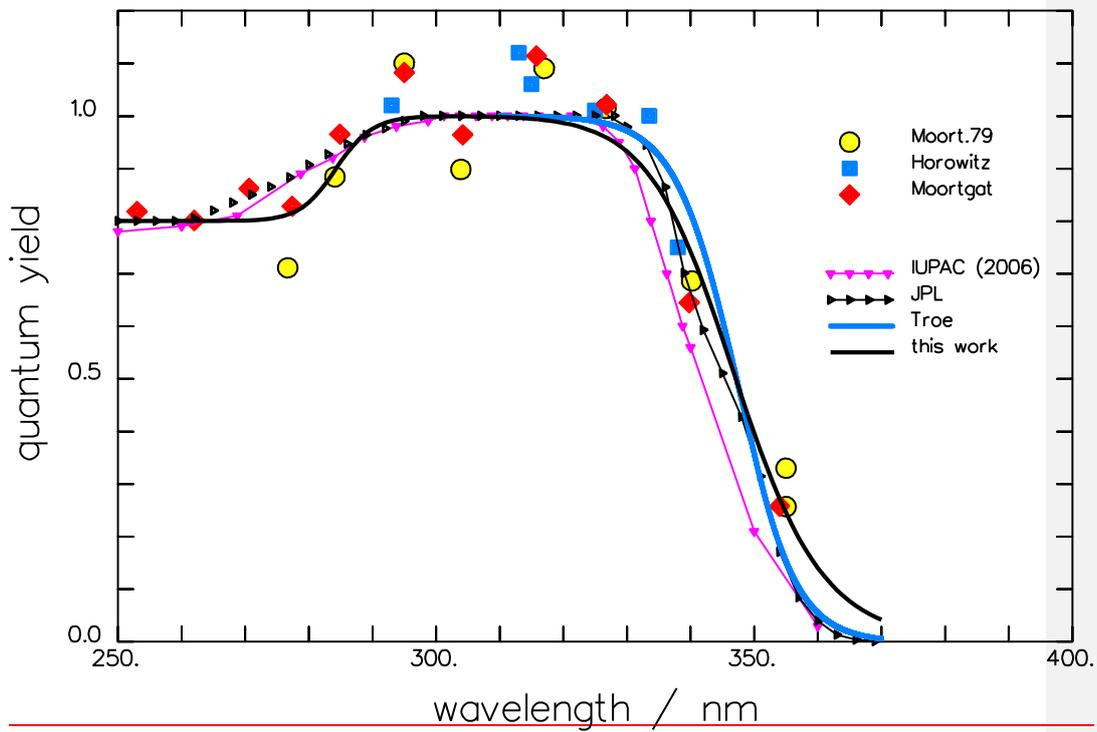
1  
2  
3  
4  
5  
6  
7  
8  
9  
10

**Figure 1:** Spectrum of the quantum yield of the radical channel of the  $\text{CH}_2\text{O}$  photolysis at room temperature. Measured data used for the fit are indicated by the large full symbols (**Horowitz** and Calvert, 1978; **Moortgat** et al., 1983; **Smith** et al., 2002; **Gorrotxategi** Carbajo et al., 2008). The present fit and the theoretical curve from **Troe** (2007) are given by full lines. Recommended data are represented by small symbols connected by a thin line: **JPL** (Sander et al., 2011); **IUPAC (2006)**, **and IUPAC (2013)**. The line structure observed by **Tatum Ernest** et al. (2012) is indicated by open circles and a dotted line.

Formatiert: Schriftart: Nicht Fett



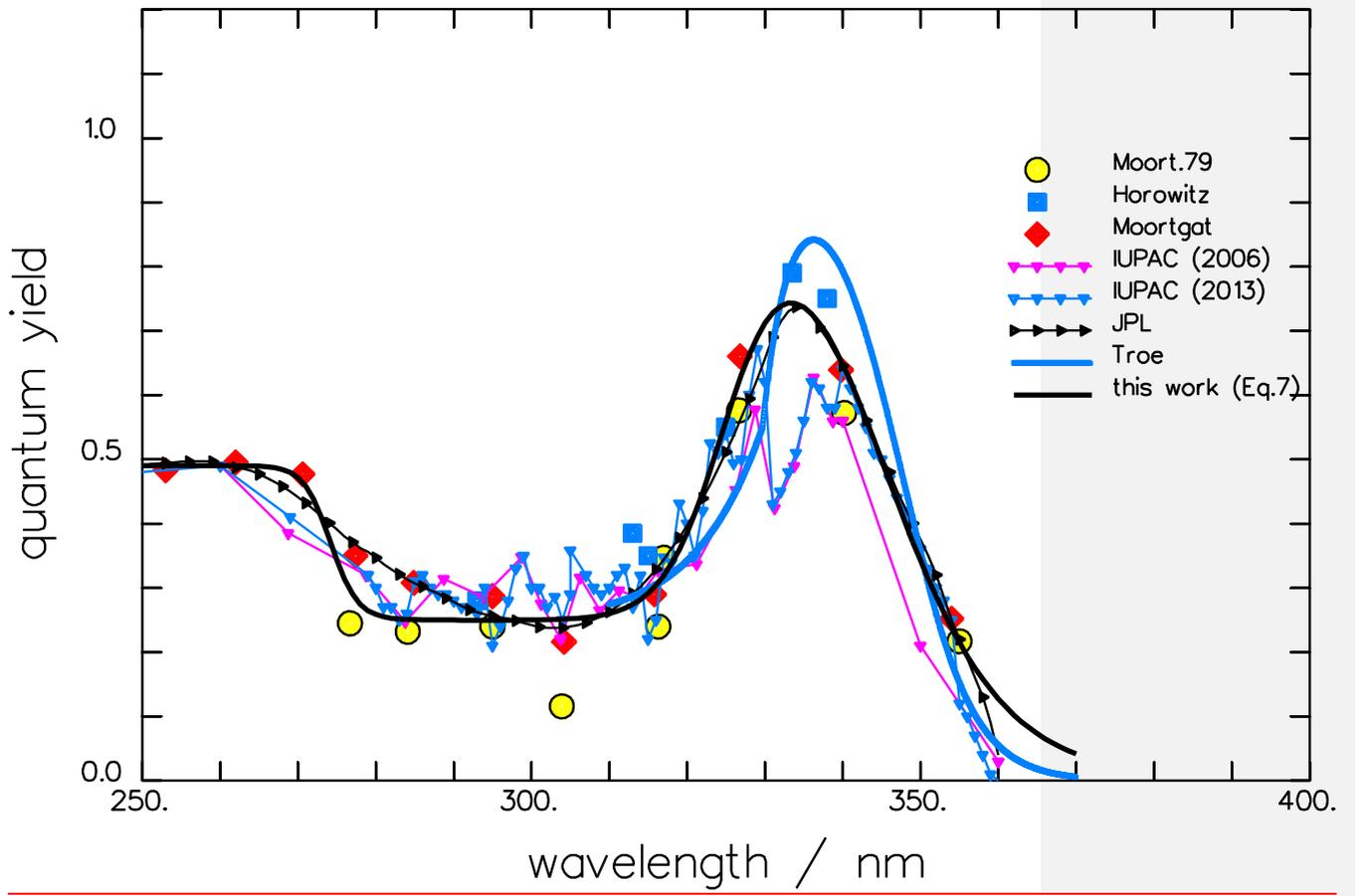
1



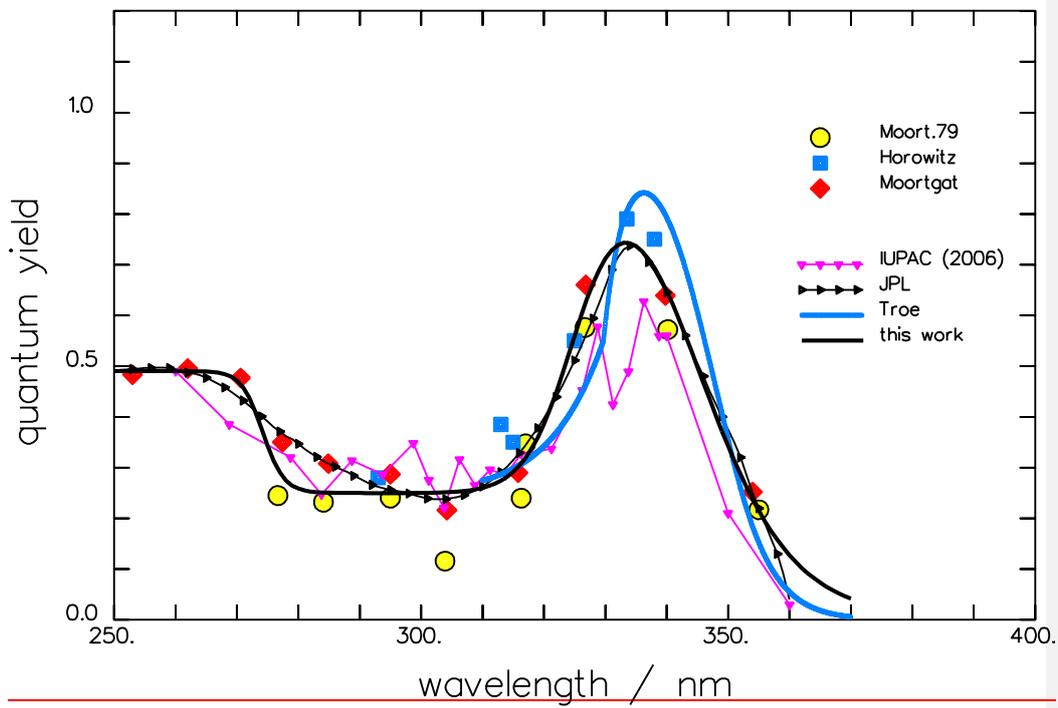
1  
2  
3  
4  
5  
6  
7  
8  
9  
10

**Figure 2:** Spectrum of the quantum yield of the total CH<sub>2</sub>O photolysis at room temperature. Measured data used for the fit are indicated by the large full symbols (**Moort.79:** Moortgat and Warneck, 1979, **Horowitz** and Calvert, 1978; **Moortgat** et al., 1983). The present fit and the theoretical curve from **Troe** (2007) are given by full lines. Recommended data are represented by small symbols connected by a thin line: **JPL** (Sander et al., 2011); **IUPAC (2006)**, **and IPUAC (2013)**.

Formatiert: Schriftart: Nicht Fett



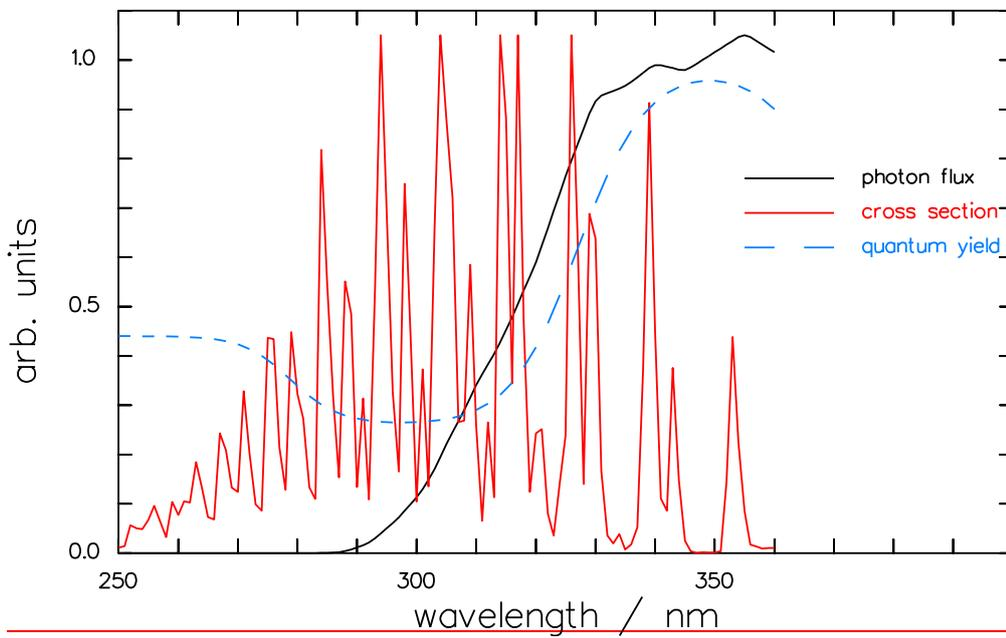
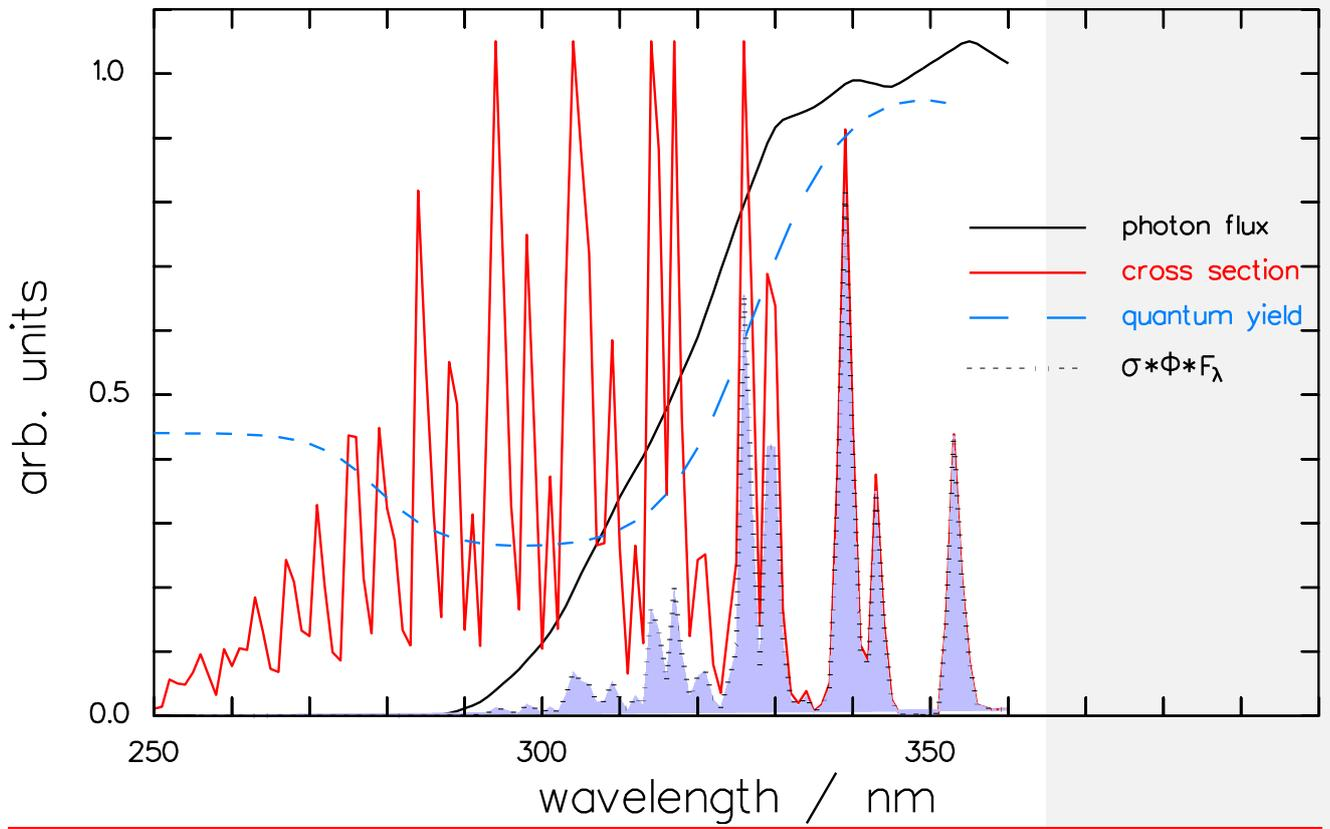
1



1  
2  
3  
4  
5  
6  
7  
8  
9  
10

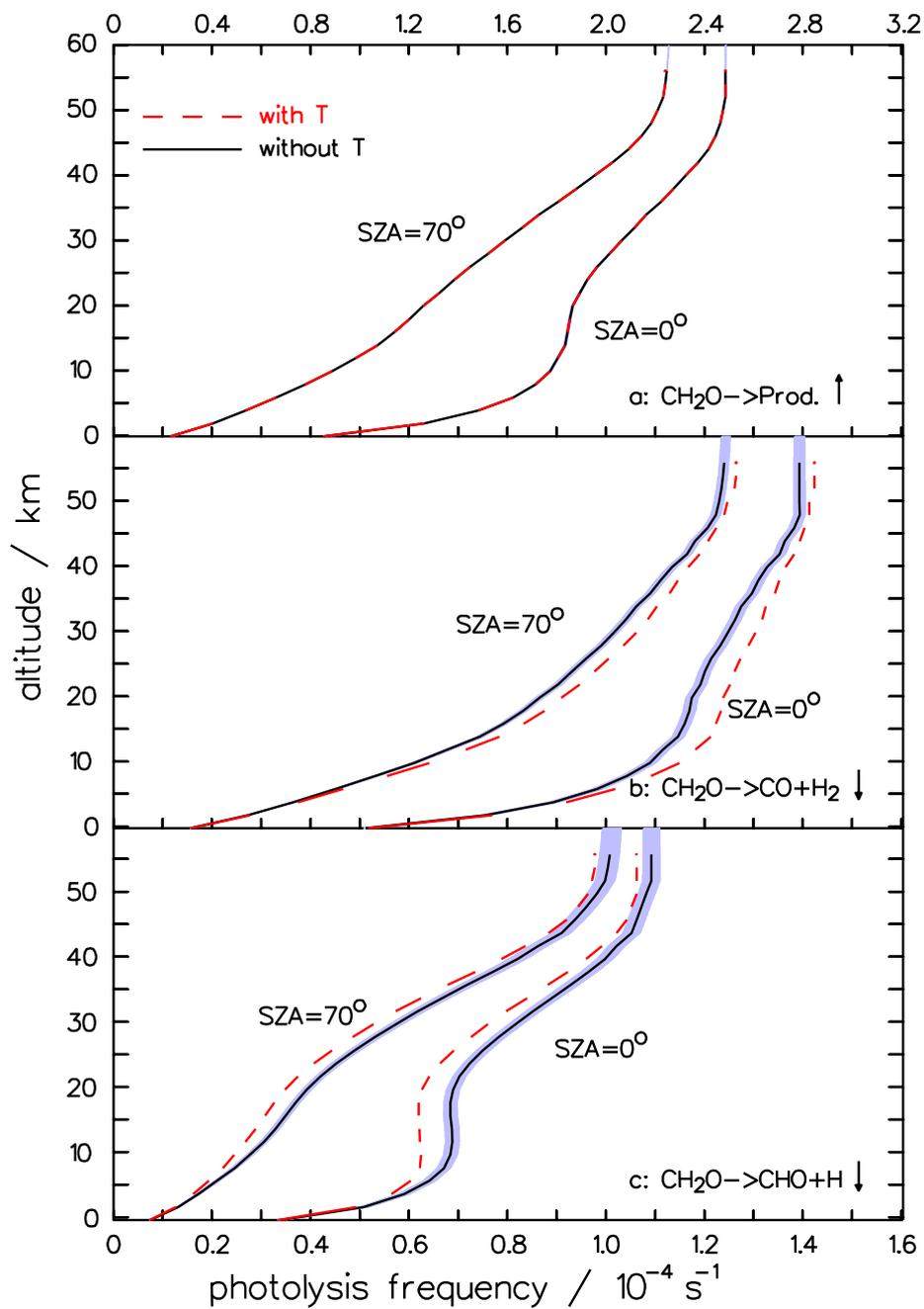
**Figure 3:** Spectrum of the quantum yield of the molecular branch of the  $\text{CH}_2\text{O}$  photolysis at room temperature. Measured data used for the fit are indicated by the large full symbols (**Moort.79**: Moortgat and Warneck, 1979, **Horowitz** and Calvert, 1978; **Moortgat** et al., 1983). The present fit and the theoretical curve from **Troe** (2007) are given by full lines. Recommended data are represented by small symbols connected by a thin line: **JPL** (Sander et al., 2011); **IUPAC (2006)**, and **IUPAC (2013)**.





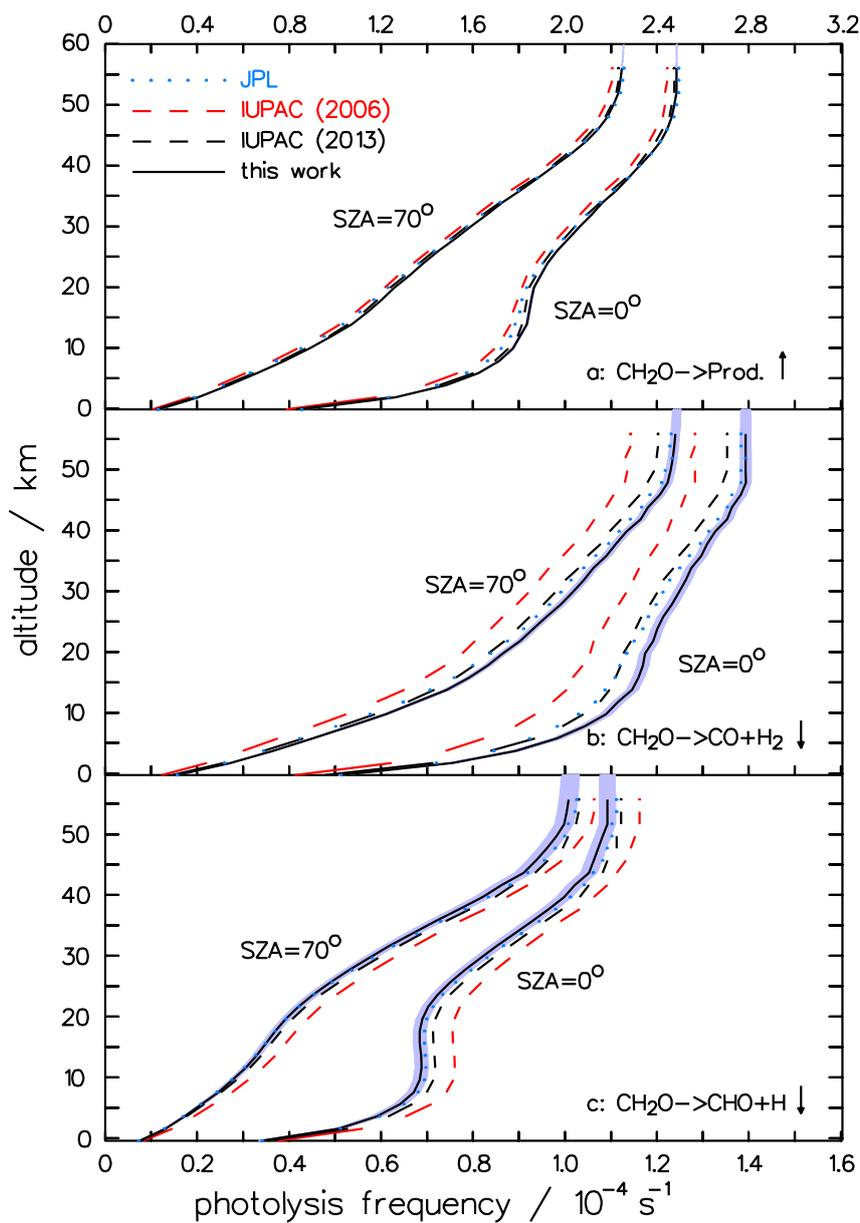
3

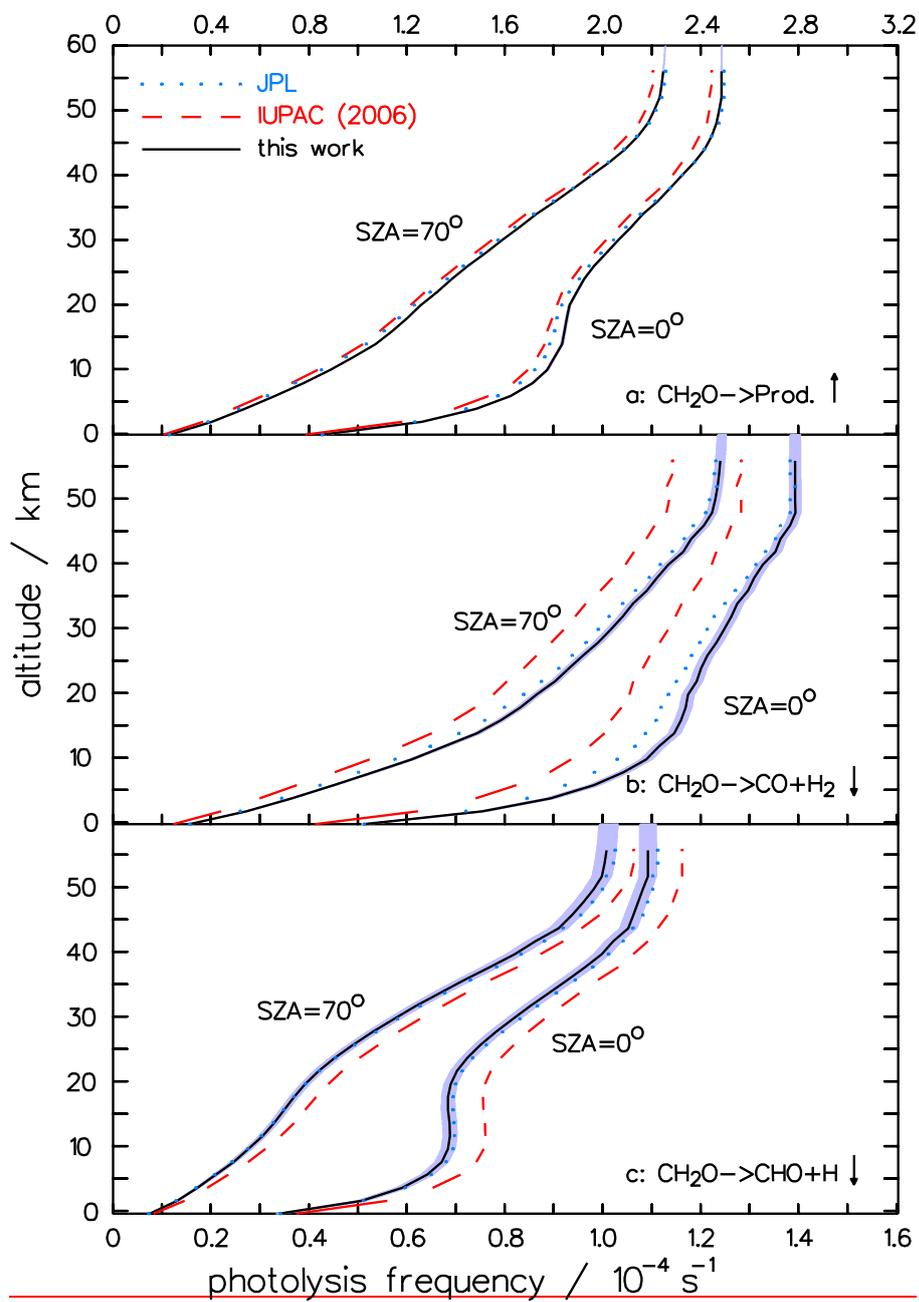
1 **Figure 4:** Spectra of the actinic photon flux density (WMO, 1985), the optical absorption  
 2 cross section (Gratier et al., 2007) and  $\Phi_{\text{mol}}$  at 30 km altitude,  $33^\circ$  solar zenith angle, 227 K.  
 3 The shaded area represents the integrand  $\sigma \cdot \Phi \cdot F_\lambda$  of Eq.(11).  
 4  
 5  
 6



7

1 **Figure 5:** Impact of a temperature dependent quantum yield,  $\Phi_{\text{rad}}$ , on the altitudinal profile of  
 2 the photolysis of formaldehyde: total photolysis (a), molecular channel (b), and radical  
 3 channel (c). The dashed line indicates the impact of the temperature dependence of  $\Phi_{\text{rad}}$  given  
 4 by Troe (2007). The shaded areas mark the  $1\sigma$  error bounds of the profiles based on the errors  
 5 of the fitting parameters for the present quantum yields. The frequencies are depicted for two  
 6 solar zenith angles (SZA). (The arrows point to the related ordinate)





1  
 2 **Figure 6:** Comparison of the altitudinal profiles of the photolysis frequencies of  
 3 formaldehyde from **JPL** (Sander et al., 2011); **IUPAC (2006)**, **IUPAC (2013)**, and the  
 4 present work: total photolysis (a), molecular channel (b), and radical channel (c). The  
 5 frequencies are depicted for two solar zenith angles (SZA). The shaded areas mark the  $1\sigma$   
 6 error bounds of the profiles based on the errors of the fitting parameters for the present  
 7 quantum yields. (The arrows point to the related ordinate)